universität wien

MASTERARBEIT / MASTER'S THESIS

Titel der Masterarbeit / Title of the Master's Thesis

„Pickering Emulsion Polymerization of Polystyrene to Synthesize Bacteria Imprinted Polymer Beads for Pre-Concentration“

verfasst von / submitted by

Martin Werner, BSc

angestrebter akademischer Grad / in partial fulfilment of the requirements for the degree of

Master of Science (MSc)

Wien, 2018 / Vienna 2018

Studienkennzahl lt. Studienblatt / degree programme code as it appears on the student record sheet:	A 066 862
Studienrichtung lt. Studienblatt / degree programme as it appears on the student record sheet:	Masterstudium Chemie
Betreut von / Supervisor:	Univ.-Prof. Mag. Dr. Peter Lieberzeit

Acknowledgements

First, I want to thank Professor Dr. Peter Lieberzeit, for giving me the opportunity to do my master thesis in his research group and for the fruitful, competent supervision during this work. I also appreciate it very much, that he enabled me to participate in the 17th International Meeting on Chemical Sensors (IMCS 2018).

Further, I want to thank Dr. Stephan Puchegger for helping me with the measurements on the scanning electron microscope. Moreover, I am very grateful to Mathias Petsovits for his support during the establishment of the measuring electronics and the data acquisition for the QCM experiments. Special gratitude goes to the whole research group of Professor Dr. Peter Lieberzeit, i.e. to Professor Dr. Dieter Baurecht, Christine Unger, Monika Marjanovic, Shahin Haghdoust, Wim Cuypers, Andrea Fischer and Felix Thier, for their steady help during this master thesis. Last but not least, I want to thank my family and friends for their long lasting support of my studies.

Frequently used Acronyms

AIBN	2,2'-Azoisobutyronitrile
APS	Ammonium Peroxidisulfate
APTES	(3-Aminopropyl)triethoxysilane
BIP-Beads	Bacteria Imprinted Polymer Beads
BPO	Benzoyl Peroxide
CFU	Colony Forming Unit
DEC	Diarrheagenic *E. coli*
DMA	N,N-Dimethylaniline
DMSO	Dimethyl Sulfoxide
DSS	Disuccinimidyl Suberate
DVB	Divinylbenzene
EbAM	N,N'-Ethylenebisacrylamide
HEMA	2-Hydroxyethyl Methacrylate
HTAB	Hexadecyltrimethylammonium bromide
LB Medium	Luria Broth Medium
MIP	Molecularly Imprinted Polymer
MISPE	Molecularly Imprinted Solid Phase Extraction
NIP	Non-Imprinted Polymer
PBS	Phosphate Buffered Saline
QCM	Quartz Crystal Microbalance
SEM	Scanning Electron Microscope
SPE	Solid Phase Extraction
TEMED	Tetramethylethylendiamine

List of Symbols

f_0	Fundamental Frequency
v_{tr}	Velocity of the Transversal Wave
d	Layer Thickness of the Quartz
Δf	Frequency Shift
Δm	Mass Change
A	Sensor Area
ρ_q	Density of the Quartz Sensor
μ_q	Shear Modulus of the Quartz Sensor
c_B	Bacteria Concentration
x	Number of Counts
F_d	Dilution Factor
RT	Room Temperature
rcf	Relative Centrifugal Force
rpm	Revolutions per Minute
C_L	Crosslinking Degree
C_M	Monomer Concentration
f	Frequency
f'	Corrected Frequency
a	Correction Factor
t	Time

Content

1. Introduction

The awareness that pathogenic microorganisms are the source of infectious diseases, is at the latest known since the pioneering work of Robert Koch on the origin of tuberculosis at the end of the 19th century [1]. However, diseases caused by bacteria are still a threat to public health. Waterborne pathogenic microorganisms, for instance, determine the sanitary risk in drinking water [2]. According to the WHO, about two million deaths per year are caused by waterborne diarrheal diseases [3]. The highest risk of water contamination by pathogenic microorganism is due to the release of feces into aquatic systems. As the variety of possibly dangerous bacteria is too vast to be directly analyzed, the water quality is determined by fecal indicator bacteria, instead. For this, the *E. coli* enumeration is an important parameter for risk assessments in water [2].

There are established methods for the detection of *E. coli*. Unfortunately, they commonly require expensive instrumentation and time-consuming analysis steps, which limits the frequency of microbial risk assessments in water samples. For this, quick and simple measuring devices, such as chemical sensors would be appreciable [4]. However, the required low detection limit - which for water quality is only one CFU per 100mL according to WHO guidelines [5] so far excludes the use of sensors for monitoring of *E. coli* under environmental conditions, as they do not feature the required sensitivity [4].

One strategy in analytical chemistry to obtain lower limits of detection for target analytes is to perform sample treatment steps before analysis. Solid phase extraction is one of the most established methods of sample preparation. To prevent co-extraction of interfering compounds, the use of selective sorbents, such as molecularly imprinted polymers, provides an effective way to pre-concentrate the analyte of interest [6]. As molecular imprinting is not only limited to small molecules, but can also be exploited to create materials with selectivity towards different bacteria species [7], it enables the opportunity to develop sorbent materials to support the detection of *E. coli*.

Polymer beads are one possible form for materials, used for molecularly imprinted solid phase extractions [8]. In order to synthesize such bacteria-selective materials, a Pickering emulsion polymerization approach, using *E. coli* as template and stabilizer of the emulsion, has already been reported to produce bacteria imprinted polymer beads [7].

Based on this, the aim of this thesis was to synthesize BIP-beads and to investigate their usability in processes of filtration and pre-concentration of the fecal indicator *E. coli*. Poly(styrene-co-divinylbenzene) was chosen to be the polymer system for the performed experiments, as styrene is a standard monomer for emulsion polymerizations [9]. The principle of the aspired system is illustrated in Figure 1. Further, the thesis aimed to combine the BIP-beads with a chemical sensor based on molecularly imprinted polymers. With this, the two most important application fields of molecular imprinting, namely solid phase extraction

and chemical sensing [10], would be coupled in order to enhance the performance of the analysis.

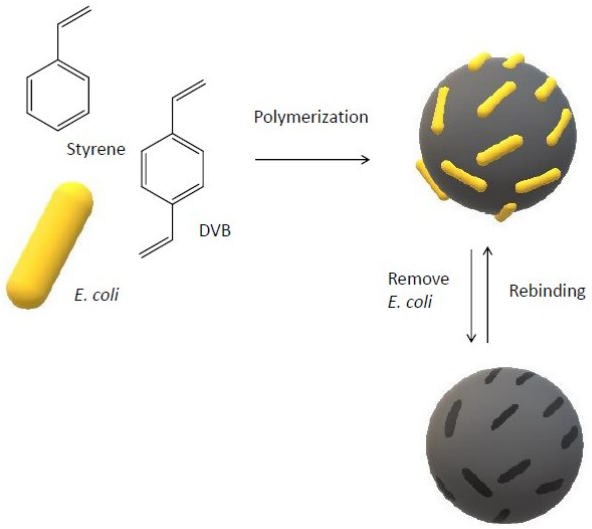

Figure 1: Pickering emulsion polymerization for *E. coli* imprinting on bead surfaces and its usability for selective binding of the bacteria [11]

Apart from the already mentioned possibilities for bacteria detection, the application of BIP-beads as transport devices in medical therapies was also examined in a part of this work. The basis of these considerations were the probiotic properties of certain bacteria strains [12]. For this, experiments, investigating the ability of *E. coli* to survive the Pickering emulsion polymerization, were performed. Viable bacteria attached to the surface of a polystyrene bead could feature a new way of microorganism transport for medical applications.

2. Theoretical Background

2.1. Pickering Emulsion Polymerization

Polymer particles can be produced using different methods such as dispersion polymerization, precipitation polymerization, emulsion polymerization or suspension polymerization [13]. Generally, the monomer phase of the polymerization is mixed with a dispersion medium, which is in many cases water. The resulting monomer droplets need to be stabilized, which is achieved through the presence of surfactants [14]. If the emulsion is stabilized by solid particles, instead of a surfactant, the process is called Pickering emulsion polymerization [15].

2.1.1. Suspension/Emulsion Polymerization

Emulsion polymerization as well as suspension polymerization is used to synthesize spherical particles during a polymerization in an emulsion. However, their underlying mechanisms as well as the resulting products are different [14].

In suspension polymerization, monomers that usually show a low solubility in water are dispersed. The resulting droplets are stabilized by a surfactant. Polymerization is triggered by a monomer-soluble initiator. Therefore, chains grow in the monomer droplets. In most cases, the underlying mechanism is free radical polymerization [13]. Suspension polymerizations typically lead to polymer beads with a size range of 50-1000µm. There is a big size distribution, which derives from the mechanical homogenization step and coalescence [14]. One important application for beads, synthesized via a suspension polymerization, is their use as chromatographic separation media [13]. The process of the suspension polymerization is illustrated in Figure 2 A.

In emulsion polymerization, hydrophobic monomers are also dispersed in aqueous phase and stabilized by surfactants. However, the initiator does not need to be soluble in the monomers. The process is then initiated in the water phase, by forming water-borne radicals. At a certain chain length, the oligomers get insoluble in water and enter so called monomer swollen micelles. These particle nuclei are supplied by the monomer droplets. The propagation reaction is performed on the particles, which were created during the initiation process [9]. The spherical product resulting from an emulsion polymerization is typically of submicron size and features a smaller size distribution as the beads obtained from a suspension polymerization process [14]. The general principle of an emulsion polymerization is illustrated in Figure 2 B.

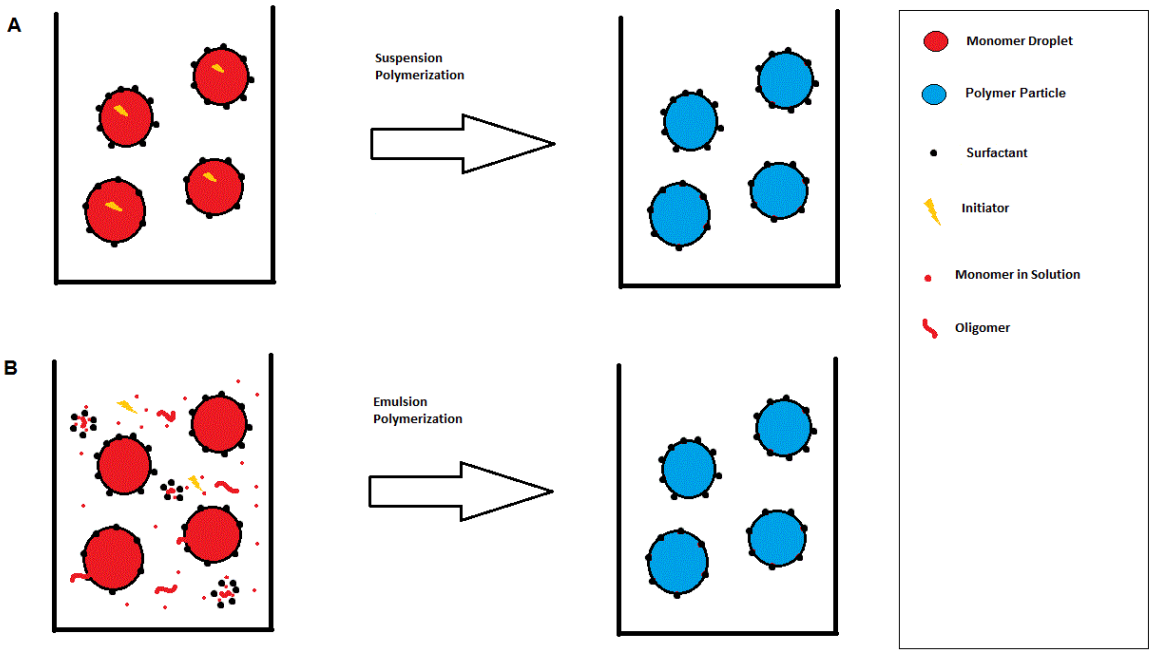

Figure 2: Schematic description of (A) suspension polymerization and (B) emulsion polymerization

As emulsions are intrinsically unstable systems, coarsening may occur. The most important mechanisms of this process are coalescence and Ostwald ripening. Coalescence is a process, in which two droplets are unified, whereas in Ostwald ripening molecules diffuse from a small droplet into larger droplets via the continuous phase [16] [17]. Both mechanisms need to be suppressed to keep the emulsion in a metastable state [16].

2.1.2. Pickering Emulsions

Pickering emulsions were first described by S. U. Pickering in 1907 [15]. In this emulsion, the dispersed droplets are not stabilized by surfactants, but by solid particles. They are located at the interface of the immiscible liquids, which prevents the droplets from coalescence [18].

Pickering emulsions have some advantaged compared to classical emulsions. Generally, they are more stable against coalescence, which makes it possible to stabilize even millimeter sized droplets [15].

There is a large variety of solid particles, which are able to stabilize emulsions. The materials can be organic as well as inorganic. Also biological compounds, like proteins, bacteria or spores can be used as stabilizers in Pickering emulsions [15].

Pickering emulsion polymerizations can be divided into water-in-oil polymerizations and oil-in-water polymerizations. Both situations lead to different products. Water-in oil Pickering emulsion can be exploited for encapsulation [19]. In the case of an oil-in-water system, the resulting products are beads [7].

2.1.3. Free Radical Polymerization of Styrene

The Polymerization of olefins, such as styrene, follows the mechanism of a free radical polymerization. Such polymerization can be initiated by various compounds [20]. One commonly used initiator for the polymerization of styrene is the azo compound 2,2'-azoisobutyronitrile (AIBN) [21]. During free radical polymerization, the decomposed initiator transfers a radical to the monomer. In the propagation phase, the polymer chain grows. Termination processes such as radical coupling or disproportion of two polymer chains stop the reaction [20]. The free radical polymerization mechanism of vinyl compounds is illustrated in Figure 3.

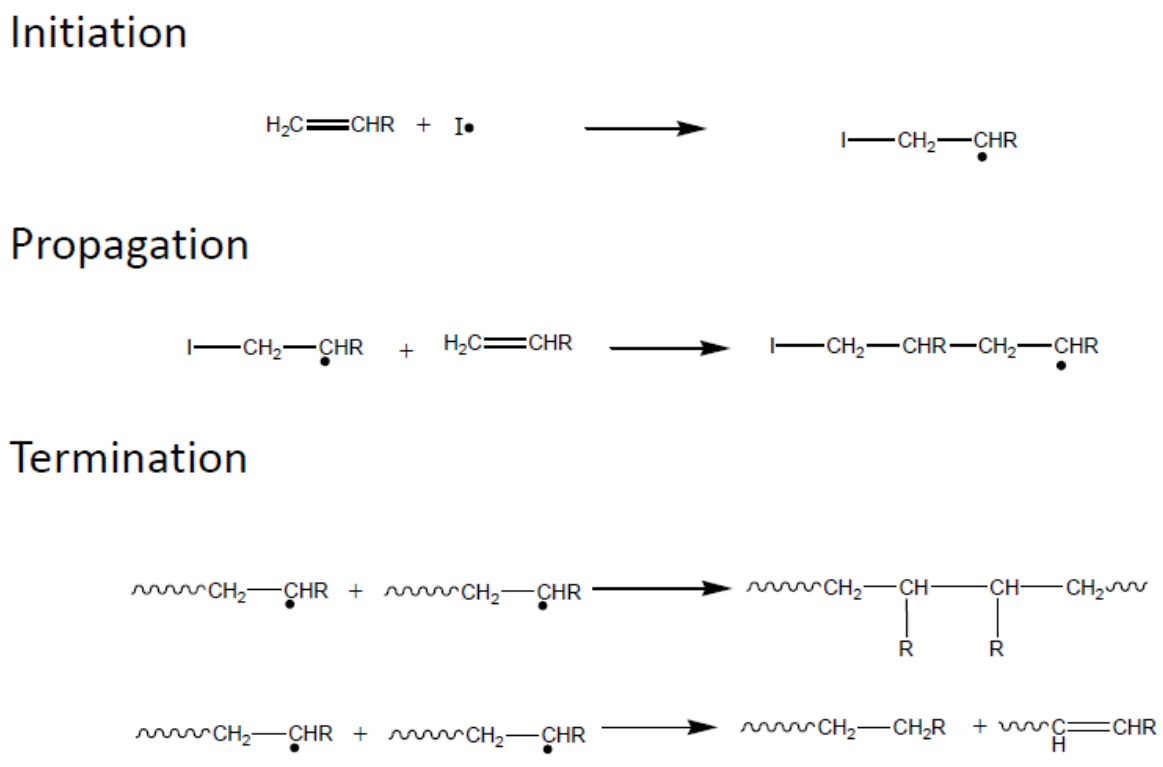

Figure 3: Mechanism of free radical polymerization

The use of cross linkers can influence the properties of the polymer. For the polymerization of styrene, divinylbenzene (DVB) can be used as a cross linking monomer [22]. Free radical polymerizations can be exploited for many polymerization strategies such as solution-, bulk-, suspension- or emulsion polymerization [20]. For emulsion polymerization styrene is a frequently used monomer [9].

The overall reaction of the free radical polymerization of styrene is illustrated in Figure 4 [20]:

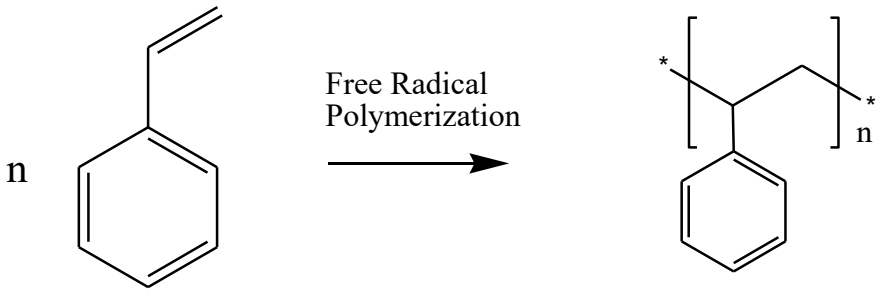

Figure 4: Free radical polymerization of styrene

2.2. Molecularly Imprinted Polymers

Molecularly imprinted polymers can be seen as artificial receptors, which mimic biological functionalities even though they are synthetic materials [23]. During molecular imprinting, cavities are formed in a synthetic polymer matrix. These cavities have complementary character towards the template molecule, which makes the MIPs synthetic receptors [24].

The process of molecular imprinting is illustrated in Figure 5. Molecularly imprinted polymers are generated by adding a template, which is the analyte for that the selective recognition is desired, to the functional monomers and cross linkers before polymerization. The polymer assembles around the template molecule. Due to the crosslinking molecules, a three-dimensional polymer structure is obtained. The template has to be removed after the polymerization, which leaves binding sites in the molecularly imprinted polymer. These cavities are complementary to the target molecules in terms of size, shape and chemical functionality [25].

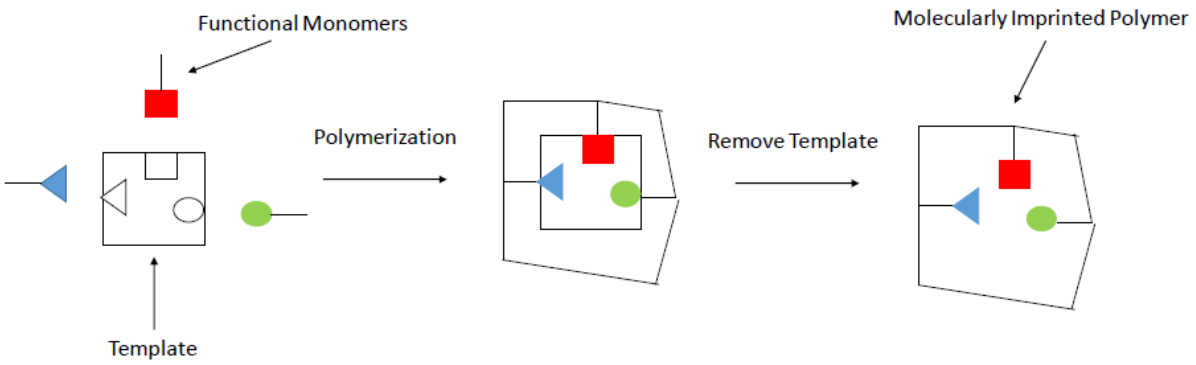

Figure 5: Illustration of molecular imprinting

Just like natural receptors, MIPs have the ability to selectively bind target analytes [25]. Binding of the analyte molecules to the cavities of the MIP occurs due to non-covalent interactions, which is another similarity of MIPs and biological recognition systems [23]. However, compared to biological compounds, MIPs have the advantage to be more robust and more resistant to temperature, pressure, organic solvents, acids and bases. Another advantage is their simple and cheap preparation [26].

The technique of molecular imprinting can be exploited for the synthesis of many different types of materials, such as hydrogels, nanofibers, spherical particles, thin films and monoliths. These materials find application in analytical chemistry, especially in the field of chemical sensing [23]. Because MIPs are selective sorbent materials, they are also inherently useful for sample treatment in processes like filtration or pre-concentration [25].

2.2.1. Bacteria as Templates for Molecularly Imprinted Polymers

Molecular Imprinting is not only limited to the selective recognition of small analytes, but also large compounds like bacteria or viruses are potential templates. However, some difficulties arise when imprinting bacteria: As they are living organisms, it is challenging to generate structurally defined cavities. Another drawback is the fact that a high cross linking ratio, which is needed in molecular imprinting, may hamper the bacteria to reach the binding sites of the MIP [7].

Different approaches for molecular imprinting of bacteria have been reported. On possibility is stamp imprinting. In this method, a stamp with bacteria on its surface patterns the polymer to form bacteria imprints [27]. Other approaches are based on a sol-gel method for the imprinting of microorganisms [28]. In Pickering emulsion polymerization, the tendency of

bacteria to be located at the oil/water interface of such emulsions is exploited for the development of recognition sites on the polymer surface [7].

2.2.2. Pickering Emulsion Polymerization for Molecular Imprinting

Pickering emulsion polymerization can be exploited for molecular imprinting. In this process, the template is located on the surface of the monomer droplets, which leads to surface imprinting during polymerization [29]. As the synthesis is carried out in droplets dispersed in a water phase, the resulting MIP beads are water-compatible. Contrary to other molecular imprinting techniques in aqueous solutions, the water molecules do not interfere with the interactions of the functional monomer and the template. The formation of molecular imprints mainly arises duo to electrostatic and hydrophobic interactions [30].

In principle, molecular imprinting in Pickering emulsion polymerization is not limited to a special kind of template. Small molecules, such as diclofenac or propranolol have been reported to be suitable for molecular imprinting in Pickering emulsion polymerizations [30] [31] as well as large biomolecules like the protein hemoglobin [29]. Even challenging templates, like microorganisms, such as *E. coli*, have been reported to be successfully imprinted using this technique [7].

However, there are different strategies for imprinting a template via Pickering emulsion polymerization: One possibility is to form a Pickering emulsion stabilized with solid particles (e.g. SiO_2 particles) and perform polymerization with the template diluted in the reaction mixture [31]. In another approach, the analyte is coated onto the solid particles, used for stabilization of the emulsion. This ensures contact of the template with the monomer droplets during the polymerization (Figure 6 B) [29]. In the case of microorganism imprinting, the behavior of bacteria to preferably assemble on the interface of the oil-water emulsion can be exploited to use these templates directly as stabilizers for the Pickering emulsion polymerization (Figure 6 A) [7].

Molecular Imprinting, performed in Pickering emulsion polymerization, features the possibility to synthesize water-compatible, stable, spherical beads with selectivity towards a desired analyte [31]. The materials synthesized during this method are mechanically highly rugged due to the fact that molecular imprinting in Pickering emulsion polymerization allows the use of a high amount of cross linker, even for large analytes like proteins or microorganisms [29] [7].

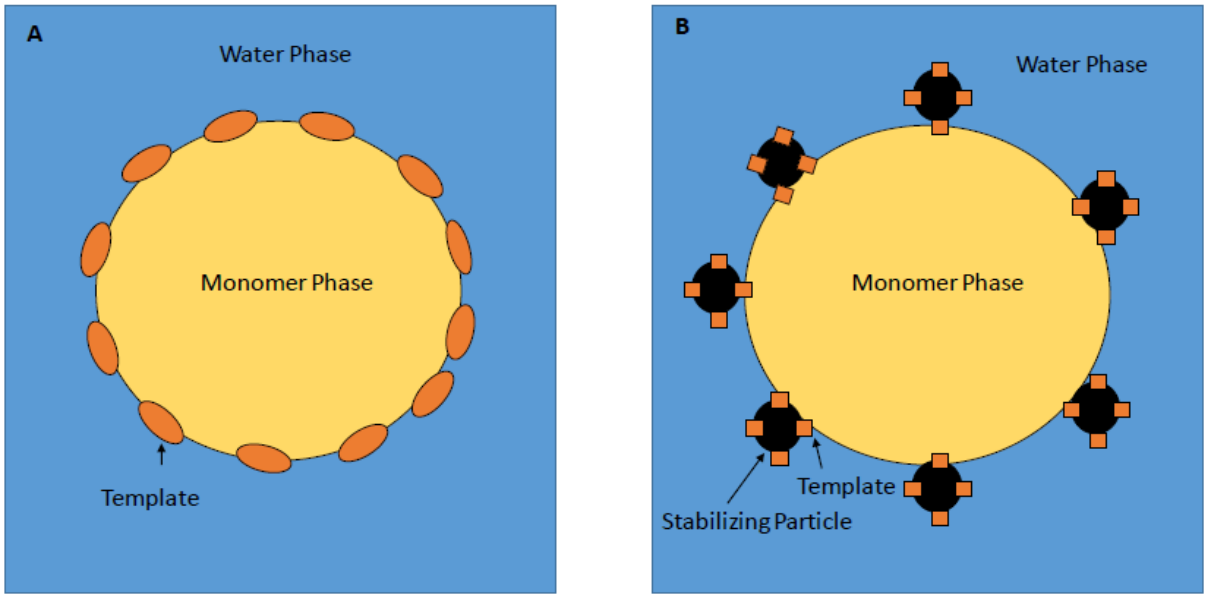

Figure 6: Strategies for molecularly imprinting in Pickering emulsion polymerizations: (A) template stabilizes the emulsion and is located at the oil-water interface; (B) stabilizing particles are coated with the template

2.2.3. Stamp Imprinting

Stamp imprinting is a frequently used technique to generate artificial recognition sites at the surface of a polymer. Generally, surface imprinting methods have the advantage that their imprints are more easily accessible for the template and therefore binding kinetics are not limited by diffusion. However, the disadvantage of this method is that fewer recognition sites are created compared to other techniques such as bulk imprinting [32].

In this molecular imprinting method, a stamp is generated by adsorbing the template molecules onto a planar surface. Frequently used materials are glass slides or silicon wafers [33]. The generated stamp is pressed onto a layer of pre-polymerized monomers until the polymer is cured. After the removal of the stamp, imprints on the polymer surface are left behind. Possibly remaining templates at the MIP can be removed by rinsing procedures [10]. The principle of the stamp imprinting method is illustrated in Figure 7.

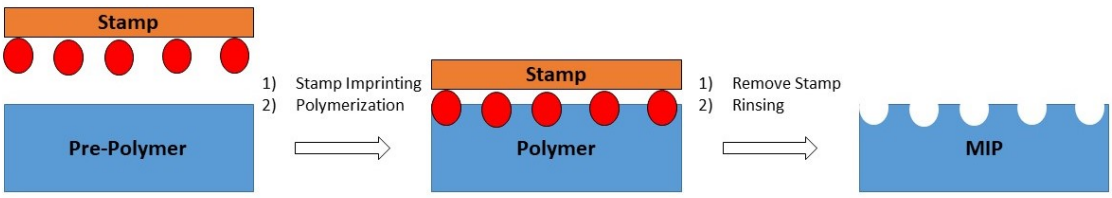

Figure 7: Schematic illustration of stamp imprinting

2.2.4. Molecularly Imprinted Solid-Phase Extraction

One crucial task in nowadays' analytical chemistry is to establish methods, capable for the detection of low analyte concentrations in the presence of a complex matrix. To yield low limits of detection, sample treatment is a necessary step in the workflow of analytical chemistry. Solid phase extraction (SPE) is a frequently used method for that purpose. One challenge in SPE is to prevent co-extraction of other compounds during enrichment of the target analyte. For this, the use of sorbents featuring selectivity to the target analyte is very important. Typical used selective sorbents are immunosorbents, mixed-mode sorbents or MIPs. However, the use of immunosorbents is limited, as they can only be used in strictly defined conditions. This is not the case for MIP sorbents, which is a big advantage [6].

Molecularly Imprinted solid phase extraction (MISPE) is one of the most used applications for MIPs [8]. Apart from MISPE, molecularly imprinted polymers are also used in MISPE related formats, such as Molecularly imprinted solid phase micro extraction (MI-SPME), Stir bar sorptive extractions and Matrix solid-phase dispersion [6][25].

MISPE can be performed in several different modes. In batch MISPE the sorbent material is incubated together with the sample. Afterwards, the sorbent material has to be removed from the sample. For this, the material is in many cases magnetic. In off-line MISPE the MIPs are placed into a cartridge. A standard SPE protocol, which involves conditioning, loading, washing and elution, is performed. The eluent can be further processed in other separation techniques (e.g. liquid chromatography). In on-line MISPE the cartridge, containing the sorbent MIP, is directly connected with a chromatographic separation column. The elution of the analyte has to be performed in the mobile phase of the chromatographic system. In the in-line MISPE approach, the solid phase extraction cartridge is directly connected to a detection system which makes it possible to perform the enrichment and extraction via MISPE as well as the determination of the analyte in one single step [25].

2.3. Biomimetic Sensors

A chemical sensor can be seen as a self-contained device, which is able to generate real-time information about analyte concentrations in a sample. Generally, such a sensor consists of a recognition element and a transducer. The duty of the recognition element is to selectively interact with the analyte. These interactions lead to the change of physical properties. The transducing element functions as a converter of the varied physical property into another easily measurable property [34]. Chemical sensors can be divided into different categories depending on the physical property, which is converted by the transducer. Important classes are electrical-, optical- and mechanical sensors [35]. In a chemical sensor, both elements are

integrated into one device [34]. The fundamental setup of a chemical sensor is illustrated in Figure 8.

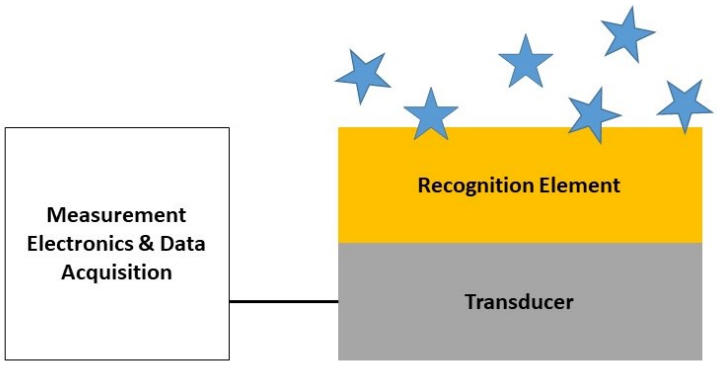

Figure 8: Principle of a chemical sensor

In a biosensor, the recognition element consists of biological compounds, such as antibodies or nucleic acids. In these sensors, specific bonds between the ligand and the recognition receptors are formed [35]. The main disadvantage of biosensors is their instability towards harsh chemical or physical conditions. To overcome this problem, biomimetic sensors can be used as an alternative. Their recognition element is an artificial material, which mimics the binding capability of biosensors in terms of affinity and selectivity. Molecularly imprinted polymers represent one possibility for biomimetic recognition elements. The binding sites of MIPs can provide comparable properties to an antibody-antigen complex in terms of affinity and selectivity [36].

2.3.1. Quartz Crystal Microbalances

The use of quartz crystal microbalances (QCMs) as mechanical sensors is a highly established technique in chemical sensing [35]. In QCMs, the piezoelectric behaviour of quartz is used to measure mass changes. For this, a thin quartz disk has to be coated with electrodes. If a potential is applied to the electrodes on the QCM, and oscillating electric field arises due to the piezoelectric properties of the quartz. This field generates an acoustic wave, which propagates through the QCM. The impedance minimum of the acoustic wave depends on the layer thickness of quartz. In the impedance minimum the layer thickness is a multiple of halve the acoustic wavelength. If the QCM is connected with an oscillation circuit, a resonance oscillation arises in the quartz [37]. The correlation between the resonance frequency and the layer thickness of the QCM is described in the following equation [38]:

$$f_0 = \frac{v_{tr}}{2 \cdot d}$$

f_0	Fundamental Frequency
v_{tr}	velocity of the transversal wave
d	Layer thickness of the quartz

The vibrational motion of the QCM at the resonance frequency can be correlated with the deposited mass at the electrodes. This correlation is described by the Sauerbrey equation [39]:

$$\Delta f = -\frac{2 f_0^2 \cdot \Delta m}{A \cdot \sqrt{\rho_q \cdot \mu_q}}$$

Δf	Frequency shift
f_0	Fundamental Frequency
Δm	Mass change
A	Sensor area
ρ_q	Density of the quartz sensor
μ_q	Shear modulus of the quartz sensor

The equation in principle describes the shift of the resonance frequency due to deposited mass. Strictly speaking, the equation is only correct if the added mass is rigidly deposited on the surface and does not slip across it [39].

It is possible to coat an array of two or more electrodes onto one quartz. If one of these electrodes functions as a reference, disturbing effects such as change in humidity, temperature or gas flow rate can be eliminated by subtracting the signal of the reference channel from the measuring channel [40].

2.3.2. Thin Film MIP as Recognition Element

In a chemical sensor based on molecularly imprinted polymers, there has to be close contact between the recognition element, which is the MIP, and the surface of the transducer. A frequently used technique is to generate a thin film of monomers on the surface of the transducer. For this, spin coating or spray coating of the monomer solution is in many cases the method of choice. This leads to an even and thin polymer layer, which can be converted by molecular imprinting into appropriate recognition elements for chemical sensors [36].

To provide suitable MIP for chemical sensing, it is important to choose the appropriate functional monomers. They must be able to form stable pre-polymers and should also be capable to interact with the target analyte in a non-covalent, reversible manner. For this, acrylate-based monomers are frequently chosen, because they can be easily polymerized and have a high variety of functionalities [41]. The acidic and basic groups of acrylate based monomers allows the MIPs to undergo columbic interactions with the template molecules [42]. Another advantage of acrylic monomers is that some of them (e.g. 2-hydroxyethyl methacrylate (HEMA)) are self-initiating, if they are irradiated by UV-light. Self-initiated photopolymerization is a meaningful approach for the design of MIPs, as it faces the idea of green chemistry and for this, provides a sustainable solution for possible industrial applications of the designed sensor [43].

2.4. Escherichia coli

The bacterial species *Escherichia coli* belongs to the genus *Escherichia*, named after the German scientist Theodor Escherich. It is a Gram-negative, facultative anaerobic bacillus, which inhabits the intestinal tract of warm-blooded animals [44]. *E. coli* is a rod-shaped bacterium, with a size of 1-3µm. The appearance of this bacterium is illustrated in Figure 9. In its cell cycle, *E. coli* propagates via cell division. In this process, bacteria cells constrict, which generates two separate cells [45].

Most *E. coli* strains are considered harmless, although some of them are pathogenic, causing diseases like diarrhea [44]. Only four strains (*E. coli* W, C, B and K-12 strain), among thousands of different isolates, are ranked in Risk Group 1 of the biological safety guidelines. They are often used for laboratory work, as they are considered non-pathogenic [46]. For some strains (e.g. *E. coli* Nissle 1917), health benefits to the host have been claimed, which demonstrates that *E. coli* can even act as a probiotic [12].

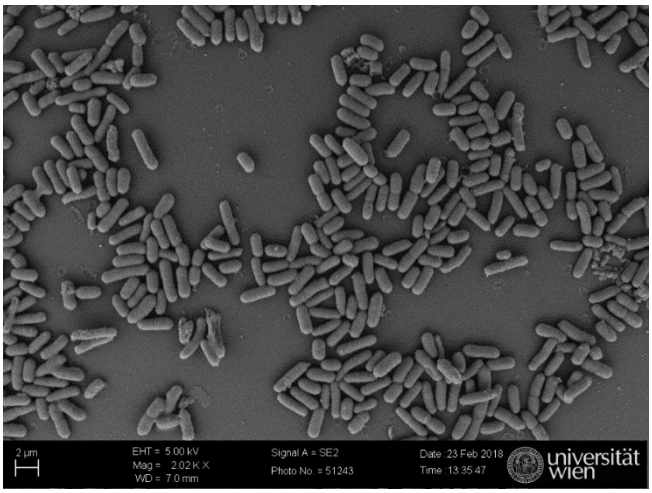

Figure 9: SEM image of *E. coli* W 9637 on a polystyrene surface

One well-known example for pathogenic strains is *E. coli* O157. Although, the reported number of infections by this strain is not very high, it is a threat to public health, as the diseases caused by *E. coli* O157 can end in the worst case with the death of the infected person [47]. Generally, the pathogenic, diarrheagenic *E. coli* (DEC) can be divided into different pathotypes. Their classification occurs according to the preferred host colonization site, the clinical symptoms after infection and the virulence mechanisms [44]. The different DEC pathotypes are listed in Table 1.

Table 1: Diarrheagenic *E. coli* pathotypes [44]

Pathotype	**Abbreviation**
Enteropathogenic *E. coli*	EPEC
Enterohemorrhagic *E. coli*	EHEC
Enteroaggregative *E. coli*	EAEC
Enterotoxigenic *E. coli*	ETEC
Enteroinvasive *E. coli*	EIEC

E. coli is an interesting analyte, because it is a fecal indicator, which helps to determine whether water is polluted or not. Bacteria, which are used as fecal indicators, have to meet several criteria: They have to be present in the excrements of warm-blooded animals and should be persistent but not able to grow in water bodies. Fecal indicators should also be easily detectable, and therefore they have to be present in relatively high concentrations [2]. In human feces, the *E. coli* concentration is reported to be around 10^8 CFU/g [48]. As *E. coli* fulfills all these criteria, its concentration is a very important parameter to predict the sanitary risk in water bodies [2].

2.5. Methods

2.5.1. Scanning Electron Microscopy

A conventional optical microscope is limited by the wavelength of visible light, which allows only magnification of about 1000x. The use of a high energy electron beam (2-1000keV) provides a much higher magnification (up to 10^6x), as the accelerated electrons have a wavelength between 0,027-0,0009nm. In a scanning electron microscope (SEM), information is obtained from detecting particles (electrons, photons) emerging from the sample surface, which is irradiated by the incident electron beam [49].

In scanning electron microscopy the incident electron beam, which is focused by lenses, scans an area of the specimen in raster mode [50]. The electron beam interacts with the surface sample and provokes radiation emerging from the specimen. These radiating particles can be captured by different detectors, which enables the SEM to collect a variety of signals by multiple detector systems [51]. The most important detectable signals are secondary electrons (SE), backscattered electrons (BSE), electron beam induced conductivity (EBIC), cathodoluminescence (CL) and x-rays [49]. The simplified working principle of a SEM is illustrated in Figure 10.

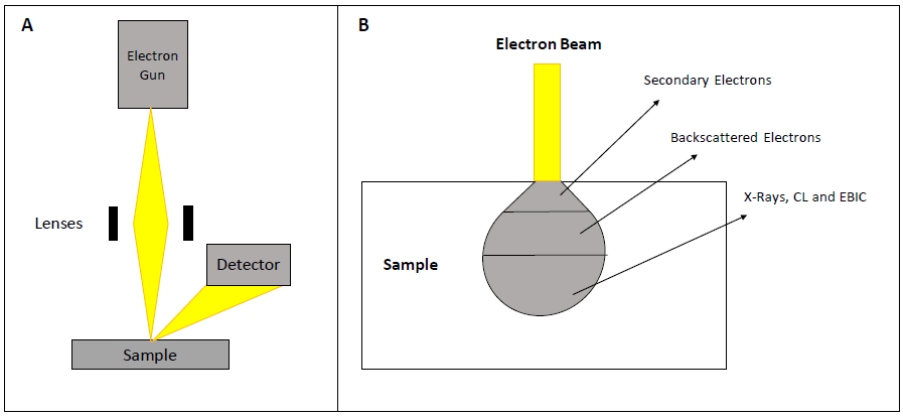

Figure 10: (A) simplified setting of a scanning electron microscope; (B) illustration of the signal generation in a scanning electron microscope

Secondary electrons arise from the specimen, as the incident electron beam knocks them out of atom orbitals in the sample [49]. The energy of such electrons is relatively low (0-50eV), which allows them to travel only short distances through the specimen. For this, secondary electrons can only be emitted from the upper part of the sample surface. The detection of secondary electrons gives information about the topography and surface chemistry of the specimen. It is the most frequently used operation mode in SEM [51]. When an incident

electron approaches an atom nucleus close enough, it is scattered through a distinct angle which allows the electron to escape from the surface. These are the backscattered electrons. They can give information about the composition and the crystallography of the specimen [49]. The operating modes for the detection of cathodoluminescence and electron beam induced conductivity are limited to semiconductor samples and therefore special applications [51].

Scanning electron microscopy requires sample preparation for insulating specimens, as surface charging would occur in such materials, which leads to interferences during examination. For this, the surface of the insulating sample has to be coated with a conductive metal layer. This can be achieved by sputtering. In this process, high voltages are applied between two electrodes in a vacuum chamber, which produces ions out of gas atoms. These positive ions can sputter target atoms out of the cathode as they are accelerated towards the electrode. These sputtered atoms can deposit on the specimen to create a conductive layer [52].

The advantages of scanning electron microscopy, compared to conversional optical microscopy, are its better magnification, a larger depth of field and the fact that it can give also information about the chemical composition, electrical properties and the crystalline structure of the specimen [49].

2.5.2. Fourier-Transformation Infrared Spectroscopy

Infrared spectroscopy is a method measuring absorption in the wavelength range of the infrared light by analyte species. The absorption of the light is due to vibrational and rotational stimulations of molecules with a dipole moment. The fact that different functional groups of a molecule absorb the light at characteristic wavenumbers can be used to obtain qualitative information. The most commonly observed vibrations are stretch- and deformation vibrations, which can be further subclassified. Stretch vibrations for instance, can be symmetric or asymmetric and deformation vibrations occur as bending, twisting wagging or rocking. The composition of different vibrational signals in an IR-spectrum enables the structural identification of the analyte, which is examined by this method [53].

A Fourier-Transformation infrared spectrometer (FT-IR spectrometer) uses a beam splitter and movable mirrors to measure the intensity in dependence of the position of the mirror. The Fourier Transformation is a mathematical method, which converts the measured signal into a sum of sinus- and cosine- functions and with this, generates an IR-spectrum of the measured sample [54]. A typical setup of a FT-IR spectrometer is illustrated in Figure 11.

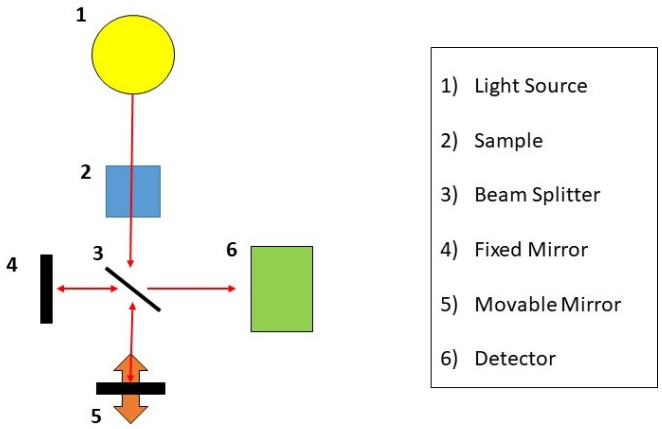

Figure 11: Setup of a Fourier-Transformation infrared spectrometer

The use of in-situ infrared spectroscopy is an established method to monitor a polymerization process. The free radical polymerization of a vinyl compound, such as styrene, can be tracked by IR-spectroscopy by looking at specific signals, which are generated or decline during the polymerization process [55].

3. Experiments

3.1. List of used Chemicals

Table 2: List of chemicals used for the experiments

Chemical	Vendor	Purity
Proteose Peptone	VWR Chemicals	
Sodium Chloride	AppliChem GmbH	99.5%
Yeast Extract	Sigma Aldrich	
D-Glucose Monohydrate	Merck KGaA	
Agarose	Sigma Aldrich	
Gram's Crystal Violet Solution	Merck KGaA	
Iodine	Fluka Chemie AG	99.5%
Potassium Iodide	Merck KGaA	
Gram's Safranin Solution	Sigma Aldrich	
Styrene	Merck KGaA	99%
Divinylbenzene	Merck KGaA	
Sodiumhydroxide	Merck KGaA	99%
Ammonium Peroxidisulfate	Fluka Chemie AG	98%
N,N-Dimethylendiamine	Merck KGaA	98%
Tetramethylethylendiamine		
Ascorbic Acid	Acros Organics	99%
Hydrogen Peroxide	Merck KGaA	35%
Benzoyl Peroxide	Merck KGaA	75%
N,N-Dimethylaniline	Merck KGaA	99%
2,2'-Azoisobutyronitrile	Sigma Aldrich	98%
Potassium Dihydrogen Phosphate	Merck KGaA	99.5%
Di-Potassium Hydrogenphosphate	Merck KGaA	98%
Hexadecyltrimethylammonium Bromide	Fluka Chemie AG	98%
Bleach (≤5% NaOCl)	DE SIMONE s.r.l.	
Acetic Acid	Carl Roth GmbH + Co. KG	99.8%
Sodium Dodecyl Sulfate	Fluka Chemie AG	90%
Methanol	VWR International	99.9%
(3-Aminopropyl)triethoxysilane	ABCR GmbH & Co. KG	
Toluene	Sigma Aldrich	99.9%
Disuccinimidyl Suberate	Thermo Scientific	
Dimethyl Sulfoxide	Merck KGaA	99.9%
Gold Paste	Heraeus GmbH & Co. KG	
2-Hydroxyethyl Methacrylate	Sigma Aldrich	99%
N,N'-Ethylenebisacrylamide	Thermo Fisher GmbH	96%

3.2. *E. coli* Cultivation

The *E. coli* bacteria used for experiments within this works were cultivated under the same conditions and stored at -20°C until they were used. The experiments were performed with the strain *E. coli* W (ATCC 9637).

3.2.1. Culture Conditions

For the cultivation of *E. coli* only previously sterilized vessels were used. The bacteria were cultivated in LB liquid medium of the following composition (Table 3):

Table 3: Composition of the LB liquid medium

Component	Concentration [g/L]
Proteose Peptone	10
NaCl	5
Yeast Extract	5
D-Glucose Monohydrate	1

The components were diluted in water followed by boiling the medium for 30 minutes. Afterwards, the LB medium was autoclaved. 20µL of an *E. coli* stock solution was transferred into 6-10mL LB medium. A previously sterilized stir bar was added. Then the bacteria were cultivated for up to 24h at 37°C. The whole process was carried out in a laminar flow hood. All instruments were sterilized by ethanol and flame contact.

After cultivation, bacteria were separated from the medium by centrifugation for 6 minutes at 1900rcf (Eppendorf Centrifuge 5702) and decantation. In the next step, the *E. coli* culture was washed two times with autoclaved water. For this, the bacteria were suspended in autoclaved water. The washing solution was removed by centrifugation for 6 minutes at 1900rcf and decantation.

3.2.2. Gram Staining

To ensure that no contamination occurred during the cultivation of *E. coli*, the produced stocks were frequently examined by Gram staining. For this, a part of the bacteria stock was transferred via a metal loop onto a glass slide. The sample was fixed onto the glass slide by rapid heating over a flame. The Gram staining procedure involves incubation steps with crystal

violet, ethanol, iodine solution and safranin. The exact incubation times and washing steps are listed in the following Table 4:

Table 4: Gram staining procedure

Component	Composition	Incubation Time [s]	Washing Steps
Crystal Violet		30	Water
Ethanol		90	
Iodine Solution	0.1g Iodine 0.2g KI 30mL water	30	Water Ethanol Water
Safranin Solution		90	Water

After Gram staining, the bacteria sample was examined under the light microscope (Nikon ECLIPSE LV100). A typical image of colored *E. coli* after staining is illustrated in Figure 12.

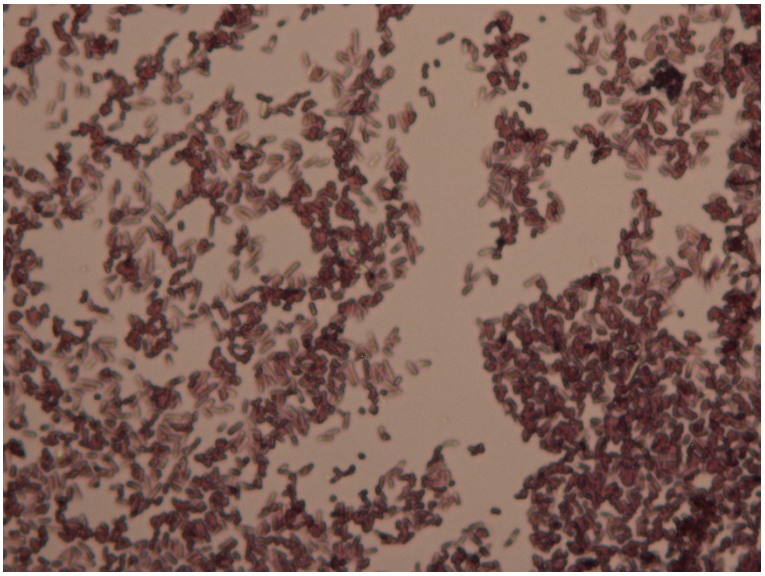

Figure 12: Image of *E. coli* W (ATCC 9637) after Gram staining

3.2.3. Cell counting

To determine the bacteria concentrations of *E. coli* samples, cells were counted in a Neubauer chamber (Counting Chamber Paul-Marienfeld GmbH & Co. KG). For this, the device was covered with a glass slide and 10µL of the bacteria sample was injected between the chamber and the glass slide. Afterwards, the bacteria were counted in 16 distinct chambers of the size 0.1mm x 0.05mm x 0.05mm. This was carried out at least two times for every sample. If the

sample was too concentrated for appropriate determination of the bacteria concentration, it had to be diluted. The *E. coli* concentration could be calculated by the following equation:

$$c_B = \frac{x \cdot 4 \cdot 10^6}{16} \cdot F_d$$

c_B	Bacteria Concentration [CFU/mL]
x	Counts
F_d	Dilution Factor

3.3. Synthesis of Bacteria-Imprinted Polymer Beads

3.3.1. Removing Stabilizer from Styrene and DVB

Commercially available monomers styrene and DVB were stabilized with 4-tert-butylcatechin, which had to be removed to improve the polymerization at the low temperature of 37°C. For this, the monomer solution was washed with an equal amount of 5% NaOH in a separation funnel. Afterwards, the monomers were washed with an equal amount of water. This procedure was carried out three times for each monomer solution. In the end, the monomer solution was several times washed with water until the washing solution revealed neutral pH. After the stabilizer was removed from styrene and DVB, these reagents were stored at 4°C.

3.3.2. Optimization of BIP-bead synthesis at 37°C

For the synthesis of bacteria imprinted polymer beads (BIP-beads), equal amounts of styrene and DVB were mixed with an initiator and a suspension of *E. coli*. The bacteria suspension was generated by dispersing the pellet of an *E. coli* culture in 4mL of distilled water. The mixture was shaken for 30 seconds to emulsify the monomer phase in the aqueous bacteria suspension. Afterwards, the reaction was carried out at 37°C.

Different initiator systems were examined due to their ability to initiate the Pickering emulsion polymerization of styrene and DVB at 37°C. For a successful BIP- bead synthesis the initiator system had to be able to produce a cured polymer without breaking the Pickering emulsion during the polymerization process. The different initiator systems are listed below:

a) Ammonium persulfate (APS) + Dimethylethylendiamine (DMEDA)
b) Ammonium persulfate (APS) + Tetramethyleethylendiamine (TEMED)
c) Ascorbic Acid + H_2O_2
d) Benzoylperoxide (BPO) + N,N-Dimethylanilin (DMA)
e) 2,2'-Azoisobutyronitrile (AIBN)

To improve the stability of the emulsion stabilized by *E. coli,* different ratios of monomer solution/ Bacteria suspension were tested during the optimization of the BIP-bead synthesis. This was mainly done for the experiments carried out with AIBN as initiator.

3.3.3. BIP-Bead Synthesis in different aqueous phases

The optimized synthesis protocol for the BIP-beads was carried out in two different aqueous phases. The exact compositions of these two synthesis protocols are listed in Table 5 below:

Table 5: Synthesis protocol of BIP-Beads in different aqueous phases

Monomer Phase	Aqueous Phase	Initiator
0.5mL Styrene 0.5mL DVB	1.2mL *E. coli* suspension in distilled water	18mg AIBN (2wt% of the monomer phase)
0.5mL Styrene 0.5mL DVB	1.2mL *E. coli* suspension in 0.1M PBS (pH=7.2)	18mg AIBN (2wt% of the monomer phase)

To generate the *E. coli* suspension, the pellet of the bacteria culture was dispersed in 4mL of distilled water or 0.1M PBS. The initiator was diluted in the monomer phase and afterwards the monomer phase was mixed with the *E. coli* suspension. The mixture was emulsified by shaking. The Pickering emulsion polymerization was carried out at 37°C over night.

The cured BIP-beads were separated from the aqueous phase by centrifugation and decantation. Afterwards, the synthesized beads were washed two times with distilled water. At the end, the beads were dried under reduced pressure. All further experiments were carried out with BIP-beads synthesized by one of these two protocols.

3.3.4. Monitoring the Polymerization of Styrene and DVB via FT-IR Spectroscopy

To monitor the polymerization of styrene and DVB initiated by AIBN, bulk polymerization was carried out. For this, 18mg AIBN were dissolved in 0.5mL styrene and 0.5mL DVB. The polymerization was carried out at 37°C in the oven. FT-IR spectra of the mixture were recorded

on PerkinElmer Spectrum100 FT-IR spectrometer before polymerization and in 1 hour intervals until 5 hours after the onset of polymerization. For this, a small amount of the mixture was transferred onto the ATR-crystal of the FT-IR-spectrometer. After the polymer was completely cured, the pulverized polystyrene was also measured at the FT-IR-spectrometer.

All spectra were measured against air as background. The transmissions of the polymerization samples were measured in the spectral range between 4000cm^{-1} – 600cm^{-1} in intervals of 0.5cm^{-1}. For each generated spectrum, the FT-IR spectrometer produced 8 scans. The used software of the PerkinElmer Spectrum100 FT-IR spectrometer was Spectrum.

3.4. Synthesis of Non-Imprinted Polymer Beads

To generate reference beads for comparing extraction efficiencies, non-imprinted polymers (NIP-beads) were synthesized. For this, 18mg AIBN was diluted in 0.5mL styrene and 0.5mL DVB. Afterwards, 1.2mL of an aqueous solution, containing 0.4g/L of the surfactant hexadecyltrimethylammonium bromide (HTAB), was added to the monomer phase. The mixture was emulsified by shaking for 30 seconds and afterwards, the NIP-beads were polymerized at 37°C until the polymer was cured.

The cured NIP-beads were separated from the aqueous phase by centrifugation and decantation. Afterwards, the synthesized beads were washed two times with distilled water. At the end, the beads were dried under reduced pressure.

3.5. Solvent Extraction for the Removal of *E. coli* from the BIP-Beads

To remove *E. coli* from the surface of the synthesized BIP-beads, different solvent extraction approaches were tested. Washing conditions were optimized in terms of used solvents, extraction time, temperature and the applying of shear forces. The different solvent extraction protocols are listed in Table 6.

The general solvent extraction procedure involved incubation of the BIP-beads in the washing solutions. Shear forces were applied either by shaking the incubated beads or by agitation with a stirring bar. After each solvent extraction step, the washing solution was removed by centrifugation and decantation. After solvent extraction, the BIP-beads were dried under reduced pressure.

Table 6: Different solvent extraction protocols to remove *E. coli* from the BIP-bead surface; RT=room temperature

Experiment Nr.	Extraction Steps	Time per Step	Temperature	Applied shear force
1	6x bleach	30 seconds	RT	shaking
2	6x 10% AcOH +1%SDS 6x H_2O 6x Methanol	30 seconds	RT	shaking
3	6x 10% AcOH +1%SDS 6x H_2O 6x Methanol	10 minutes	37°C	stirring
4	6x 10% AcOH +1%SDS 6x H_2O 6x Methanol	10 minutes	0°C	stirring
5	1x 10% AcOH +1%SDS 6x H_2O 1x Methanol	24 hours for 10%AcOH + 1%SDS and Methanol; 1 hour for H_2O	RT	stirring

3.6. *E. coli* Viability after the Pickering Emulsion Polymerization

3.6.1. Preparation of LB-Agar Plates

The LB-agar plates, which were used to test the viability of *E. coli* after different Pickering emulsion polymerization approaches were produced under sterile conditions. The composition of the LB-agar medium is listed in Table 7 below:

Table 7: Composition of the LB-agar medium

Component	Concentration [g/L]
Agarose	15
Proteose Peptone	10
NaCl	5
Yeast Extract	5
D-Glucose Monohydrate	1

The components were diluted in autoclaved water; the mixture was cooked for 30 minutes for sterilization. Afterwards, 10mL of the LB-agar medium was transferred into sterile petri dishes.

To ensure the sterility of the LB-agar plates, they were incubated for a certain time at 37°C. As no cell growing was observable, they could be used for the viability tests.

3.6.2. Pickering Emulsion Polymerization Approaches for Bacteria Viability

Pickering emulsion polymerizations were performed in sterile vessels using only sterile aqueous phases to ensure that positive viability tests did not derive from contaminations. To synthesize BIP-beads under conditions, which ensures the viability of the bacteria during the polymerization process, Pickering emulsion polymerization approaches with different aqueous phases were carried out. The different approaches are listed in Table 8 below:

Table 8: Different Pickering emulsion polymerization approaches for *E. coli* viability tests

Monomer Phase	Initiator	Aqueous Phase	Repetitions
0.5mL Styrene + 0.5mL DVB	18mg AIBN	*E. coli* suspension in water	1
0.5mL Styrene + 0.5mL DVB	18mg AIBN	*E. coli* suspension in glucose solution (1g/L)	1
0.5mL Styrene + 0.5mL DVB	18mg AIBN	*E. coli* suspension in LB-medium	4

The *E. coli* suspension was generated by suspending the pellet of an *E. coli* liquid culture in 4mL of the particular aqueous phase. In all polymerization approaches, the reaction mixture was incubated at 37°C until the BIP-beads were cured.

3.6.3. Viability Tests on LB-Agar Plates

The viability tests were carried out in a laminar flow hood. Only sterilized items were allowed to get in contact with the synthesized BIP-beads. The reaction mixture, containing the cured beads, was centrifuged for 2 minutes at 600rcf to separate the aqueous phase from the beads. 100µL of each aqueous phase was spread onto a LB-agar plate. Afterwards, the solution was decanted and the BIP-beads were washed two times with autoclaved water by centrifugation (2 minutes 600rcf) and decantation. A part of the beads was spread onto a LB-agar plate. The rest of the synthesized BIP-beads was dried in a sterile petri dish and afterwards spread onto LB-agar plates. With this, every polymerization approach was tested three times to its ability to preserve the *E. coli* bacteria in a viable state:

a) *E. coli* viability in the aqueous phase
b) *E. coli* viability on the beads after washing
c) *E. coli* viability on dried beads

The LB-agar plates, containing the test substances of the different polymerization approaches were incubated for up to 48h. The incubation time was ended, if CFUs deriving from viable *E. coli* were clearly observable. For plates with positive viability tests, Gram staining was performed to ensure that CFUs did not derive from contaminations. A schematic description of the viability test performed is illustrated in Figure 13.

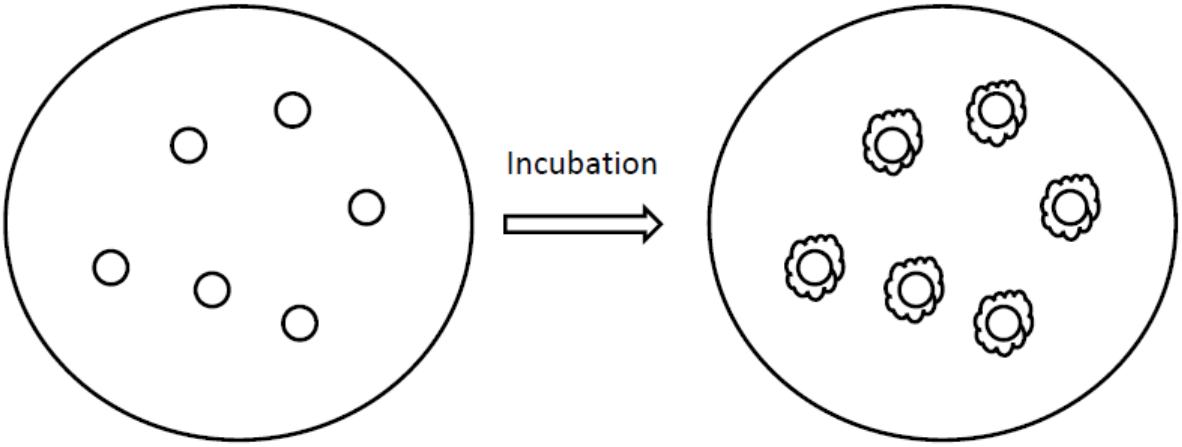

Figure 13: Scheme of the viability test for E. coli after the Pickering emulsion polymerization; in this case, a positive viability test is illustrated

3.6.4. Viability Test in LB- liquid culture

To examine the ability of BIP-beads to induce propagation of viable *E. coli* in a liquid culture, dried beads of a previously positive tested approach were incubated for 48 hours in LB-liquid medium at 37°C under agitation. Afterwards, the cultivated bacteria were separated from the medium and washed with autoclaved water as described before. Gram staining was performed to ensure, that the CFUs did not derive from contaminations.

3.7. *E. coli* Rebinding Experiments

To examine the ability of the BIP-beads to rebind *E. coli* onto the surface, experiments were carried out in bacteria suspensions of water and 0.1M PBS (pH=7.2). The *E. coli* concentration for the rebinding experiments was adjusted to 3 x 10^8 CFUs/mL. The used BIP-beads derived from the Pickering emulsion polymerization approach with water as aqueous phase. Solvent extraction was carried out previously to the rebinding experiments, to generate BIP-beads without *E. coli* attached to its surface.

For the rebinding experiment, 5mg of BIP-beads were incubated for 25 hours in 1mL of the corresponding *E. coli* suspension. During the incubation, the samples were stored at 4°C. Afterwards, the suspension was completely removed and the beads were dried at 37°C. In one experiment carried out in 0.1M PBS, the BIP-beads were additionally washed by rinsing two times with water.

The ability of the BIP-beads to rebind *E. coli* on their surface was only qualitatively investigated in these experiments by characterizing the bead surface with the SEM.

3.8. Surface characterization with the Scanning Electron Microscope

Scanning electron Microscopy was the method of choice to characterize the BIP-beads. With this, the success of the Pickering emulsion polymerization, the efficiency of the solvent extractions and the ability to rebind *E. coli* onto the bead surface was controlled.

To prepare the samples for the investigation under the SEM, they were put onto a carbon tip, which was placed on top of a sample holder. Afterwards, the sample was sputtered with 5nm gold layer (Leica EM SCD050 sputtering device), which was necessary, because polystyrene beads are insulating materials.

All samples were characterized by the Zeiss Supra 55 VP Scanning Electron Microscope. The standard settings for the SEM were an acceleration voltage of 5kV, a working distance of about 7mm and an aperture size of 30µm. All measurements were carried out with the SE2 detector.

3.9. Fabrication of an *E. coli* QCM-Sensor based on MIP

The fabrication of a QCM-sensor, capable for the sensing of *E. coli* was based on a previously optimized protocol [56]. The designed sensor was based on an acrylate polymer, which was converted into an *E. coli* sensitive recognition element by molecular imprinting:

3.9.1. Electrode Screen-Printing

Electrodes were screen printed onto quartz wavers with a diameter of 14mm and a resonance frequency of 10MHz. During that process the quartz wavers were covered with templated sieves comprising the electrode structure. Afterwards, gold paste was deposited through the sieves to layer the wavers with the designed gold electrode structure. The top- and the bottom side of the quartz were screen printed separately with different electrode geometries. The in house manufactured template sieves are illustrated in Figure 14.

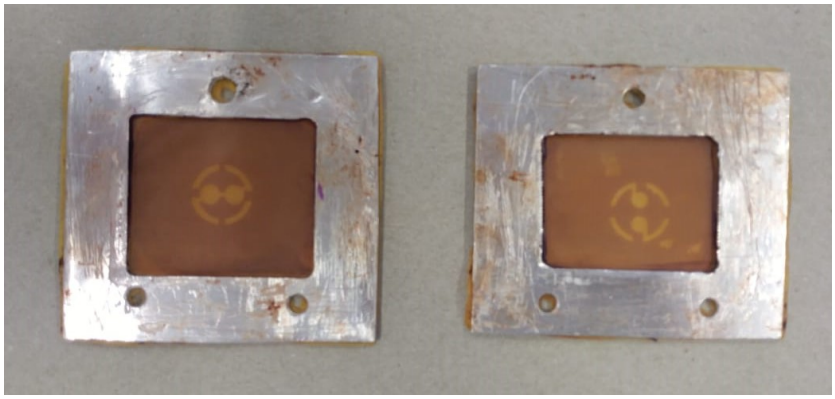

Figure 14: Template sieves for screen-printing of gold electrodes onto quartz wavers; the left sieve is for the top side of the QCM and the right sieve is for the bottom side of the QCM

After, screen-printing the gold paste onto the quartz layer, the QCM was baked for 4 hours at 400°C (Heraeus thermicon P oven). This generated a fixed gold electrode layer in the desired electrode geometry onto the waver surface. A QCM, manufactured by this method, is illustrated in Figure 15. After the fabrication, all QCMs were tested towards their usability at the network analyzer (Agilent E5062A). Only those with a damping above -5dB were used for the production of sensors (i.e. in a range from 0dB to -5dB).

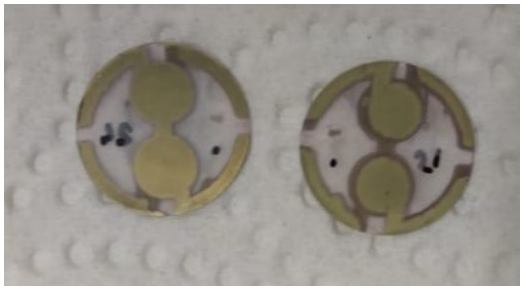

Figure 15: QCMs with screen-printed electrodes; on the left QCM, the top side is captured; on the right QCM, the bottom side is captured

3.9.2. *E. coli* Stamp fabrication

Molecularly imprinted polymers on the respective QCM surfaces were deposited by stamp imprinting. For this, stamps were manufactured that covalently bound *E. coli* template.

Glass slides were cut into an appropriate size to cover the QCM electrodes, i.e. roughly 5x5mm^2. They were cleaned in ethanol by ultra-sonication. Afterwards, they were incubated for 3 minutes in a solution containing (3-aminopropyl)triethoxysilane in toluene (191µL APTES in 10mL toluene). In the next step, the glass slides were cleaned by rinsing water three times over their surface. After the stamps had been dried, they were incubated for 1 hour in a disuccinimidyl suberate / dimethyl sulfoxide solution (5g/L DSS). In the next step, the glass slides were cleaned by rinsing three times 25mM PBS solution over their surface and subsequently dried again. At this point, the glass surface was capable to covalently bind bacteria onto its surface. For this, the stamps were covered with 50µL of a concentrated *E. coli* PBS solution (ca. 10^9 CFU/mL *E. coli*; 25mM PBS) and incubated for 2 hours. To remove the bacteria which had not bound to the stamp surface, the glass slides were rinsed with water. The stamps were dried at 37°C and stored at 4°C, until they were used for stamp imprinting.

To check the success of the *E. coli* binding onto the stamp surface, every used stamp was investigated under the light microscope (Nikon ECLIPSE LV100). Only glass slides revealing appropriate bacteria density were accepted for stamp imprinting. An example for a stamp with a typical *E. coli* density used for the sensor manufacturing is illustrated in Figure 16.

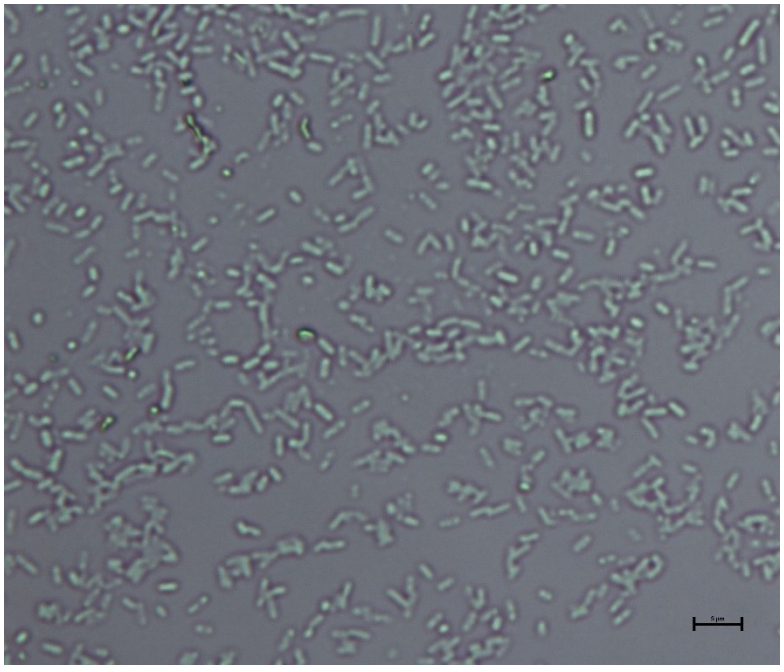

Figure 16: Light microscopy image of a manufactured *E. coli* stamp

3.9.3. Generation of MIP layers

All sensor layers were based on a molecularly imprinted polymer consisting of Poly(2-(hydroxyethyl)methacrylate-co-N,N'-ethylenebisacrylamide). For this, the monomer 2-hydroxyethyl methacrylate and the cross linking monomer N,N'-ethylene(bisacrylamide) were diluted in 25mM PBS buffer. The aimed crosslinking degree was C_L = 65% and the aimed monomer concentration was C_M = 7.5%. The appropriate concentrations were calculated by the following formulae:

$$C_L = \frac{n(EbAM)}{n(EbAM) + n(HEMA)} = 65\%$$

$$C_M = \frac{m(HEMA + EbAM)}{m(PBS) + m(HEMA + EbAM)} = 7.5\%$$

Taking the purity of the used chemicals into account, the required reaction mixture consisted of 23.4mg HEMA and 58.6mg EbAM diluted in 1mL 25mM PBS (pH = 7.0). To ensure complete dissolution of the monomers, the mixture was sonicated for 15 minutes in an ultrasound bath. Afterwards, oxygen was removed from the solution by purging 15 minutes with argon gas. The self-initiating character of HEMA was exploited to pre-polymerize the reaction mixture for 10 minutes under UV light (λ = 312nm). The generated pre-polymer was used to fabricate thin films on QCM electrodes. For this, 20µL of the reaction mixture was transferred onto each electrode and the QCM was spin coated for 30 seconds at 750rpm (Spincoat G3P-8, Specialty Coating Systems). Afterwards, polymerization of the thin film polymer on the electrodes propagated for further 20 minutes under UV-light (λ = 312nm). The QCM was again spin coated for 10 seconds at 2000rpm. In the next step, the electrode, which was chosen to be the MIP-electrode, was covered with the fabricated *E. coli* stamp, whereas the other electrode (NIP-electrode) was covered with a clean glass slide. To ensure successful imprinting, pressure was applied to the stamps to press it into the polymer thin film. The Polymer was cured over night at 50°C.

At the end, the stamps were removed from the QCM and the quartz was washed in water. The fabricated sensor was characterized at the network analyzer (Agilent E5062A) to investigate the change of the damping and the shift of the resonance frequency due to the coating of the polymer onto the QCM electrodes.

3.9.4. QCM Measurements

The setup for QCM-sensor measurements consisted of a measuring cell connected to a frequency counter (Agilent 53131A 225Hz Universal Counter), an oscillation circuit, and a power supply. Data processing of the measured frequencies was achieved by in-house scripted measuring software (based on Python). The manufactured QCM was placed into the measuring cell, in a way that the MIP-electrode as well as the NIP-electrode were connected to separate electrode contact channels. The sensitive side of the sensor faced the upper side of the cell to be exposed to the respective sample. The measuring cell was closed by a PDMS lid, which ensured that only the top side of the QCM could be in contact with the measuring solution. An image of the in-house fabricated measuring cell is illustrated in Figure 17.

During the measuring, the solutions were exchanged by injections of the new solution through the tubes in the PDMS lid. At the beginning of each measurement, distilled water was filled into the measuring cell. The polymer layer on the electrodes was allowed to swell completely in water before the measurements started. For the measurements of the different *E. coli* samples, 200µL of the solution were injected. After the sensor response achieved stable signal, the measuring cell was flushed at least two times with distilled water. When the sensor signal stabilized again after the washing step, a new sample could be injected.

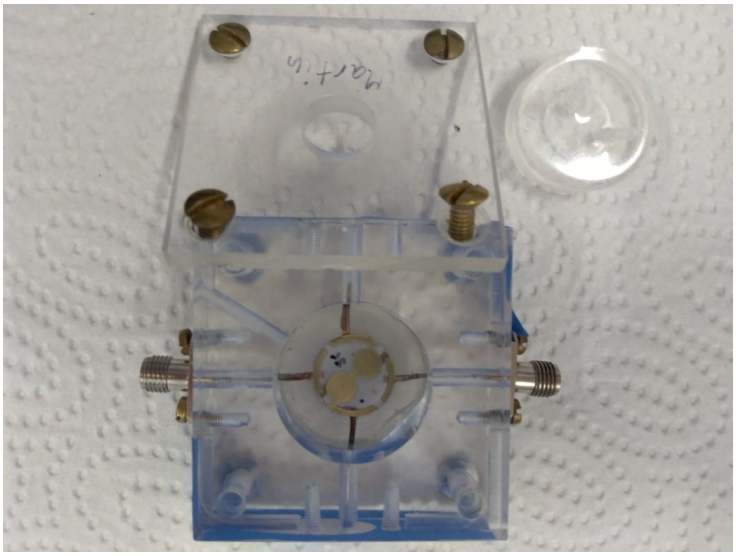

Figure 17: Picture of a QCM measuring cell connected to a QCM; the PDMS lid and the cover are placed next to the measuring cell

3.10. Filtration Experiments

The ability of the BIP-beads to filtrate *E. coli* in a bacteria solution was investigated on a column packed with BIP-beads. In these experiments, only BIP-beads synthesized in 0.1M PBS as aqueous solution were used. *E. coli* was previously removed from the bead surfaces by solvent extraction. Filtration efficiency was determined via measurements with the fabricated *E. coli* sensitive QCM-sensor. To investigate, if the filtration effect derives from the imprints on the bead surface, the same experiments were also carried out with a NIP-bead packed column.

For the filtration experiments a glass pipette served as column. Cotton wool was placed on the outlet of the column to prevent the beads to be flushed out. On top of the cotton wool, the glass pipette was packed with 500mg of the beads. Filtration efficiency was investigated for a *E. coli* suspension of 2 x 10^8 CFUs/mL. For this, 1mL of the bacteria suspension was injected onto the column. The solution was eluted by applying pressure with a Peleus ball, which was placed on top of the column. The filtrated sample was collected and measured at the QCM measuring device.

4. Results and Discussion

4.1. Bacteria Imprinted Polymer Beads

4.1.1. Pickering Emulsion Polymerization with Different Initiator Systems

Various initiator systems were tested to synthesize BIP-beads via Pickering emulsion polymerization at 37˚C. The success of synthesis was assessed based on the ability of the initiator system to polymerize the monomer phase without breaking the emulsion. To increase stability of the emulsion, different ratios between monomer and aqueous phase were tested. The results of the different experiments are listed in Table 9.

Table 9: Results of the different Pickering emulsion polymerization experiments at 37°C

Monomer Phase	Aqueous Phase	Initiator System	Emulsion Stability	Polymeri-zation	Comments
100µL Styrene + 100µL DVB	800µL *E. coli* suspension	8mg APS + 4mg DMEDA	stable	no	
100µL Styrene + 100µL DVB	800µL *E. coli* suspension	4mg APS + 2.5µL TEMED	flocculation	yes	Polymerization did not occur in the monomer droplets
100µL Styrene + 100µL DVB	800µL *E. coli* suspension	8mg APS + 5µL TEMED	flocculation	yes	Polymerization did not occur in the monomer droplets
100µL Styrene + 100µL DVB	800µL *E. coli* suspension	12mg APS + 7.5µL TEMED	flocculation	yes	Polymerization did not occur in the monomer droplets
500µL Styrene + 500µL DVB	4mL *E. coli* suspension	2.2mg Ascorbic Acid + 20µL H_2O_2 (30% w/v)	stable	no	
500µL Styrene + 500µL DVB	4mL *E. coli* suspension	5.0mg Ascorbic Acid + 40µL H_2O_2 (30% w/v)	stable	no	
500µL Styrene + 500µL DVB	2mL *E. coli* suspension	20mg AIBN	not stable	yes	Gram straining revealed unhealthy *E. coli*
500µL Styrene + 500µL DVB	2mL *E. coli* suspension	40mg AIBN	not stable	yes	Gram straining revealed unhealthy *E. coli*
500µL Styrene + 500µL DVB	1.2 mL *E. coli* suspension	18 mg AIBN	stable	yes	Successful synthesis of BIP-beads
500µL Styrene + 500µL DVB	1.2 mL *E. coli* suspension	8mg BPO (purity=75%) + 12.5µL DMA	stable	yes	Was not able to form a cured polymer
500µL Styrene + 500µL DVB	1.2 mL *E. coli* suspension	8mg BPO (purity=75%) + 31.3µL DMA	stable	yes	Was not able to form a cured polymer

The first experiments were based on typical redox initiator systems such as APS/TEMED and BPO/DMA, as they were reported to initialize polymerizations at low temperatures [57]. However, the Pickering emulsion polymerization experiments based on APS/TEMED did not lead to polymerization inside the monomer droplets. Interestingly, flocculation occurred during synthesis, which indicates that polymerization might have occurred in the aqueous phase. One explanation for this could be the fact that APS is a water soluble initiator [58]. For this, polymerization is likely to occur in the aqueous phase but not in the monomer droplets.

The experiments carried out with the oil soluble redox initiator system BPO/DMA [58] revealed that it is indeed possible to polymerize the monomers inside the droplets. However, this initiator system turned out unsuitable to produce cured polystyrene beads. The resulting beads were of gel-like consistence and therefore not useful.

As the typical redox initiator systems did not lead to successful BIP-bead synthesis, experiments were also performed with ascorbic acid/H_2O_2, which is a rather unusual redox initiator system [59]. However, in these experiments no polymerization at all was observable.

Successful synthesis of BIP-beads via a Pickering emulsion polymerization at 37°C was achieved with the oil soluble initiator AIBN [58]. However, the stability of the emulsion during these experiments had to be improved. For this, the volume of the aqueous phase was decreased. Furthermore, care was taken that a healthy *E. coli* stock was used to stabilize the emulsion. The optimized oil/water ratio to ensure the stability of the emulsion was 1 part monomer phase to 1.2 parts *E. coli* suspension. Concerning the amount of used initiator, it turned out that 2wt% AIBN was feasible to initialize the Pickering emulsion polymerization at 37°C.

4.1.2. Impact of the Aqueous Phase on BIP-Bead Synthesis

BIP-bead synthesis was performed in *E. coli* water suspension as well as in *E. coli* suspension in 0.1M PBS (pH 7.2). Both approaches turned out feasible to form polystyrene beads with bacteria attached onto the surface. The SEM images of both sets of experiments are shown in Figure 18 and Figure 19, respectively.

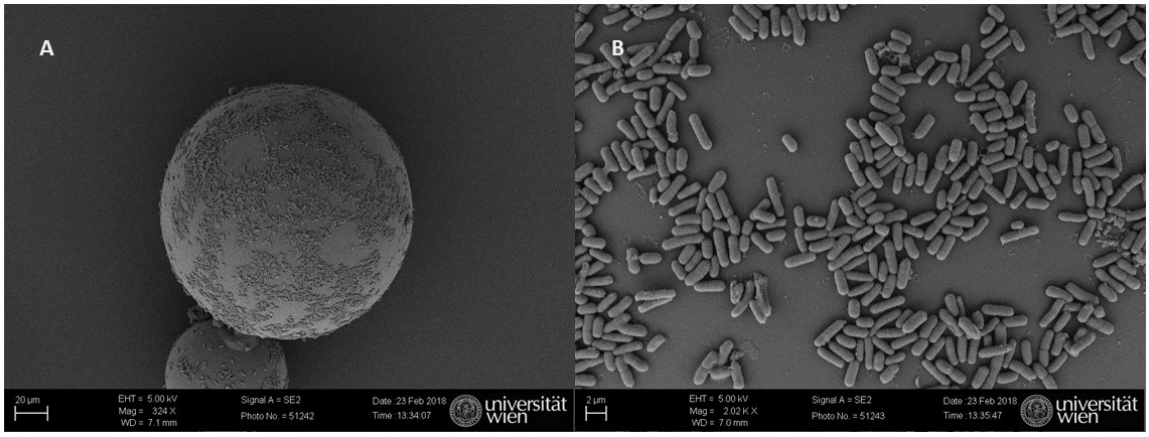

Figure 18: SEM image of BIP-beads synthesized in aqueous *E.coli* suspension as the aqueous phase: (A) image illustrates a BIP-bead; (B) image illustrates the *E. coli* attached to the surface of a BIP-Bead

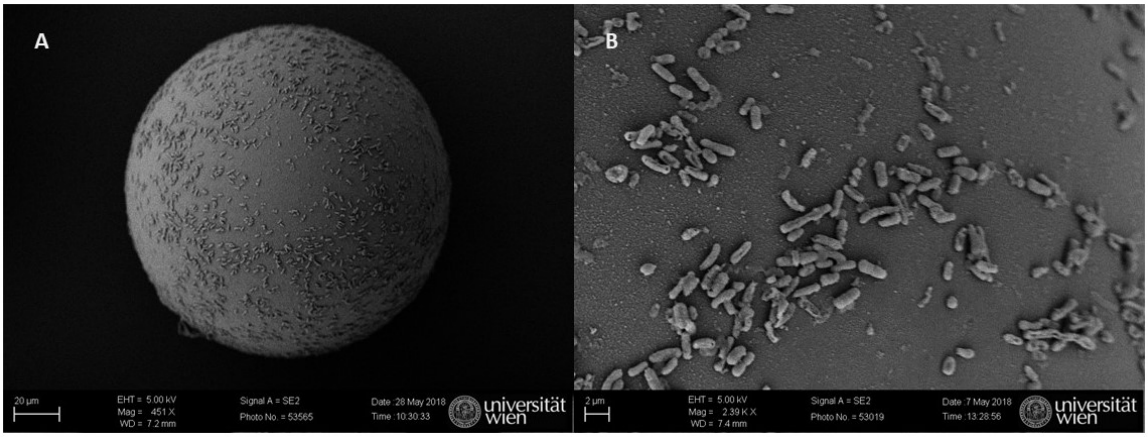

Figure 19: SEM image of BIP-beads synthesized in an *E.coli* suspension using 0.1M PBS as aqueous phase: (A) image illustrates a BIP-bead; (B) image illustrates the *E. coli* attached to the surface of a BIP-Bead

Scanning electron microscopy revealed that both synthesis approaches produced beads with bacteria attached to their surfaces. However, one important difference is the amount of bacteria loaded onto the beads surface, which was higher for BIP-beads polymerized in *E. coli* water suspension. This is an advantage, as bigger bacteria coverage of the surface potentially leads to more imprints after solvent extraction.

It is also clearly observable that the shape of the bacteria differs between both approaches: *E. coli* attached to the surface of beads synthesized in water are slightly bigger and have a more uniform appearance than the bacteria on the surface those synthesized in PBS. In favourable environmental conditions, the osmolarity in the cytoplasm of the bacteria is higher than the osmolarity of the environment, which generates a form-stabilizing pressure on the cell wall. If the ionic strength of the bacteria surrounding solution is increased, the pressure drops, which leads to water efflux. Such a hyperosmotic shock has an influence on the cell size and shape [60]. For this, the observed alteration in the *E. coli* cell shape and size can be

explained by the comparably high ionic strength of the 0.1M PBS solution in which the bacteria were suspended.

Regarding size distribution of the synthesized beads, SEM revealed that the beads were in a size range of a few micrometres up to several hundred micrometres. BIP-beads synthesized in PBS solution were altogether smaller than those synthesized in water. A qualitative overlook of the size distribution is illustrated in Figure 20.

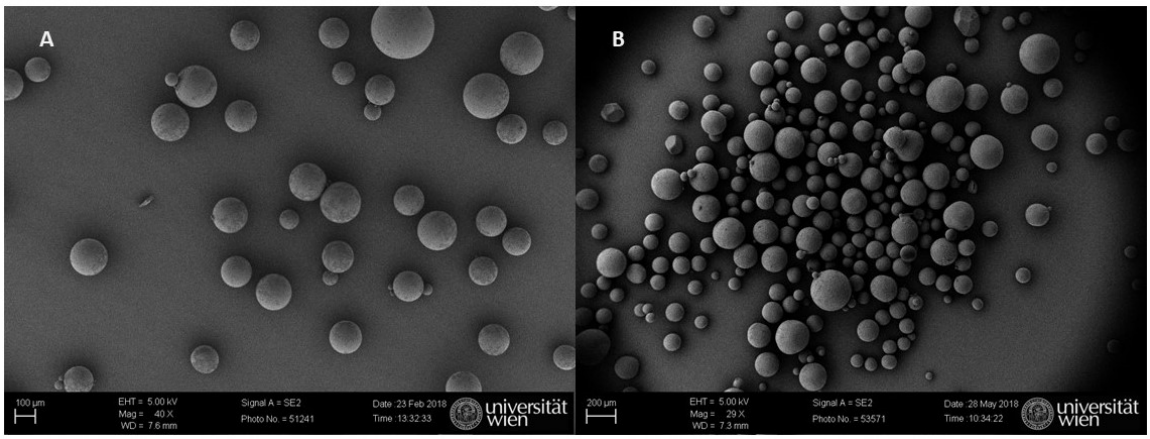

Figure 20: SEM images revealing an overlook of the size distribution of BIP-beads: (A) BIP-beads synthesized in water; (B) BIP-beads synthesized in 0.1M PBS

4.2. Non-Imprinted Polymer Beads

To obtain a reference to the BIP-beads, polystyrene beads without imprinted *E. coli* were synthesized. HTAB turned out feasible to stabilize the emulsion of styrene and DVB in water. Scanning electron microscopy images of the synthesized NIP-beads are illustrated in Figure 21.

Although the surface of the NIP-beads was rather smooth, some particulate structures were observable there. These depositions could derive from the surfactant HTAB, as the stabilizing molecules assembled at the surface of the droplets during polymerization. The overall size of the NIP-beads was smaller than the BIP-beads. This demonstrates that although *E. coli* is feasible to stabilize the emulsion of styrene and DVB in water, it is not as efficient as a surfactant.

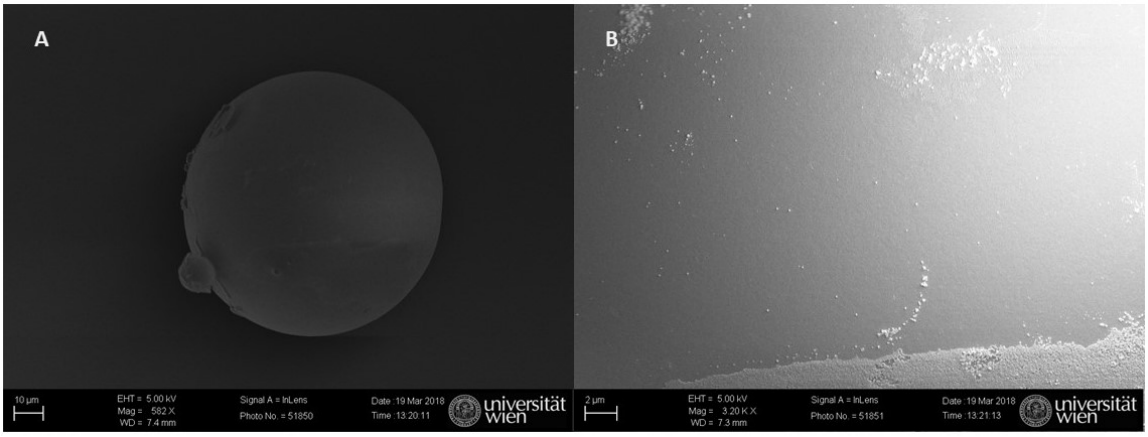

Figure 21: SEM images: (A) of a NIP-bead; (B) of the NIP-bead surface

4.3. FT-IR Investigation of Styrene/DVB Polymerization

To follow the polymerization of polystyrene beads, FT-IR-spectroscopy was used at different times during a bulk polymerization approach. The measured spectra during the first 5 hours of the polymerization are collected in Figure 22.

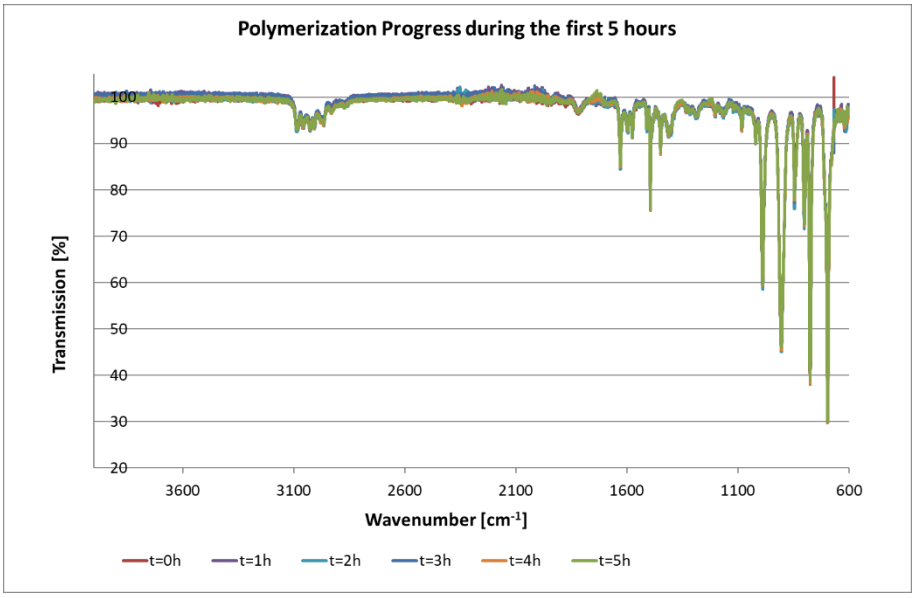

Figure 22: Polymerization progress during the first 5 hours of the batch polymerization of styrene and DVB initiated by 2wt% AIBN; the reaction temperature was 37°C

At first glance, FT-IR-measurements do not reveal a detectable change in the composition of the reaction mixture, as the spectra did not feature any alteration during the first 5 hours of the polymerization, even though the system reached its gel point after 4 hours. The success

of the polymerization could only be demonstrated due to investigations of the spectra difference between the monomer mixture and the obtained, cured polymer at the end of the reaction. The measured FT-IR-spectra are collected in Figure 23.

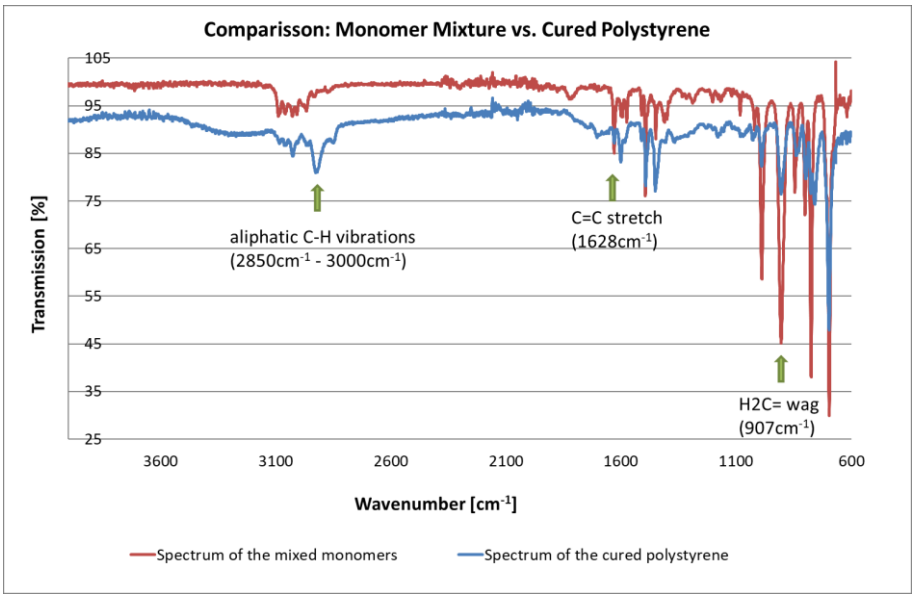

Figure 23: Comparison of the FT-IR-spectra of the mixed monomers and the cured polystyrene. Spectral regions of special interest (C=C stretch; H_2C= wag; aliphatic C-H vibrations) are marked with arrows

To interpret the results of the comparison between the spectrum of the monomer mixture and the cured polymer, the change in three distinct spectral regions has to be taken into account: During polymerization H_2C=CH- groups of both styrene and DVB are converted into an aliphatic carbon chain [20]. Hence spectral bond intensities of the double bond (C=C stretch at 1628cm^{-1}; H_2C= wag at 907cm^{-1}) have to decline during polymerization, whereas signals between 3000cm^{-1} – 2850cm^{-1} – aliphatic stretch vibrations - have to appear due to the formation of the polymer backbone [55]. Exactly this behaviour was observed in the comparison of the spectrum measured in the monomer mixture and the spectrum of the cured polymer.

4.4. Removal of *E. coli* from BIP-Beads

To remove *E. coli* efficiently from the surface of the BIP-beads, the solvent extraction protocol required optimization. For this, different influence factors were screened to enhance extraction efficiency.

4.4.1. Solvent Extraction with commercial bleach

One approach was carried out in commercial bleach, comprising NaOCl concentration of ≤5%. The ability to remove bacteria from the bead surface was examined by SEM (Figure 24).

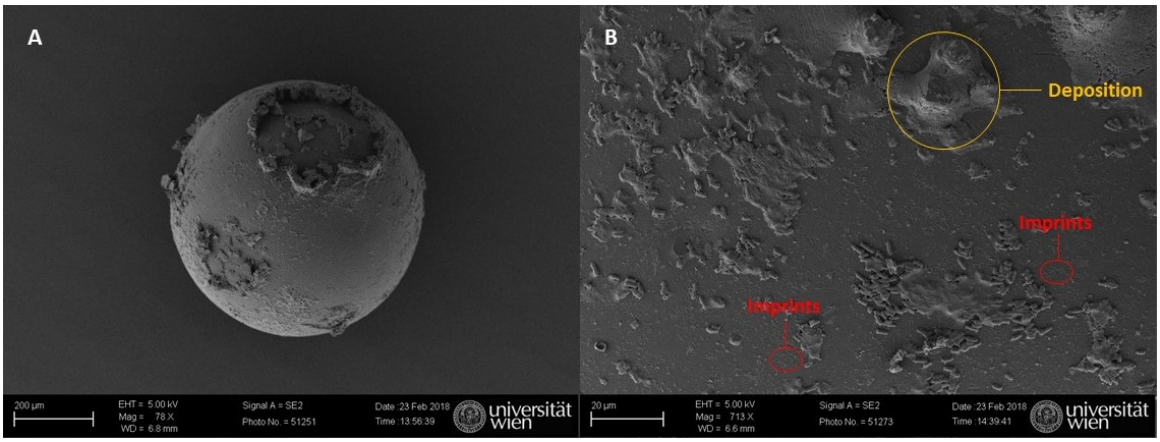

Figure 24: SEM image of a BIP-bead after solvent extraction in commercial bleach: (A) image of the bead; (B) image of the bead surface (imprints are marked with red, deposition is marked with yellow)

SEM investigation of the BIP-bead surfaces after solvent extraction revealed that it was possible to partly remove *E. coli* from the bead surface, leaving imprints behind. However, many undesired depositions, which derive from the used solvent, occurred during this extraction experiment. For this, the protocol was not feasible to produce useful BIP-beads.

4.4.2. Solvent Extractions Combining Different Solvents

As the use of a combination of different solvents was already reported to remove bacteria efficiently from synthesized BIP-beads based on a N-acrylchitosan polymer [7], the procedure was adapted for the poly(styrene-co-divinylbenzene) based BIP-beads to increase the efficiency of the process. The procedure consisted of 6 extraction steps in aqueous solution of 10% acetic acid + 1% SDS, followed by 6 extraction steps in water and 6 extraction steps in methanol. To support removal of *E. coli*, shear forces were applied by shaking. The results of the SEM investigation of the BIP-beads after solvent extraction are illustrated in Figure 25.

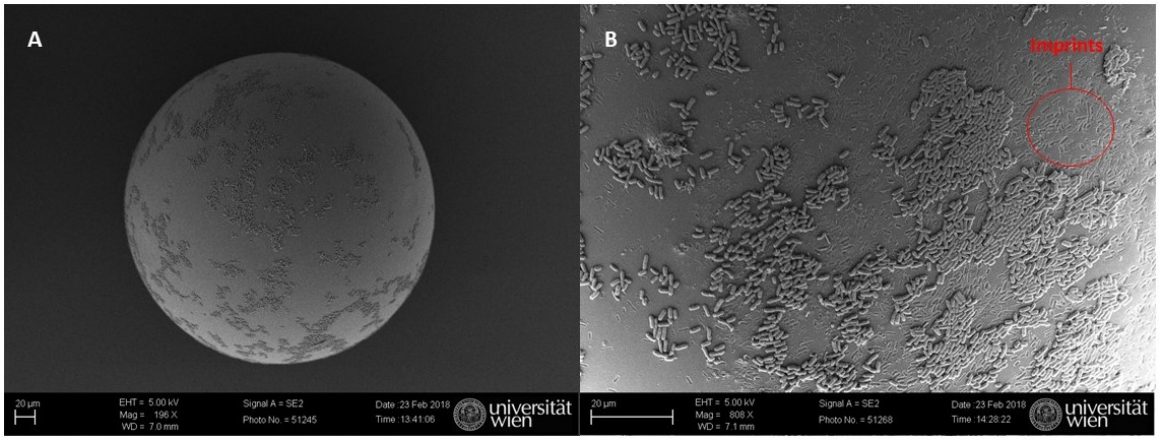

Figure 25: SEM images of a BIP-bead after solvent extraction in 10% AcOH + 1% SDS, H_2O and methanol: (A) image of the bead; (B) image of the bead surface (imprints are marked with red)

Scanning electron microscopy revealed that this solvent extraction approach was indeed feasible to remove a high amount of bacteria from the bead surface. The obtained BIP-beads featured bacteria and imprints coexisting on the surface. No other depositions were observable. However, this approach did not lead to BIP-beads, which would be useful for bacteria filtration or pre-concentration, as it was not possible to remove *E. coli* completely. Nevertheless, the combination of these solvents turned out promising. Therefore, following solvent extraction optimizations were based on them.

4.4.3. Influence of Shear Forces, Extraction Time and Temperature

Three parameters of the solvent extraction were modified to further improve the bacteria removal (The results of the experiments are illustrated in Figure 26 and Figure 27):

1) Shear forces: Agitation instead of shaking
2) Extraction time: Increased to 10 minutes for each step
3) Temperature influence: Solvent extractions at 37°C and 0°C

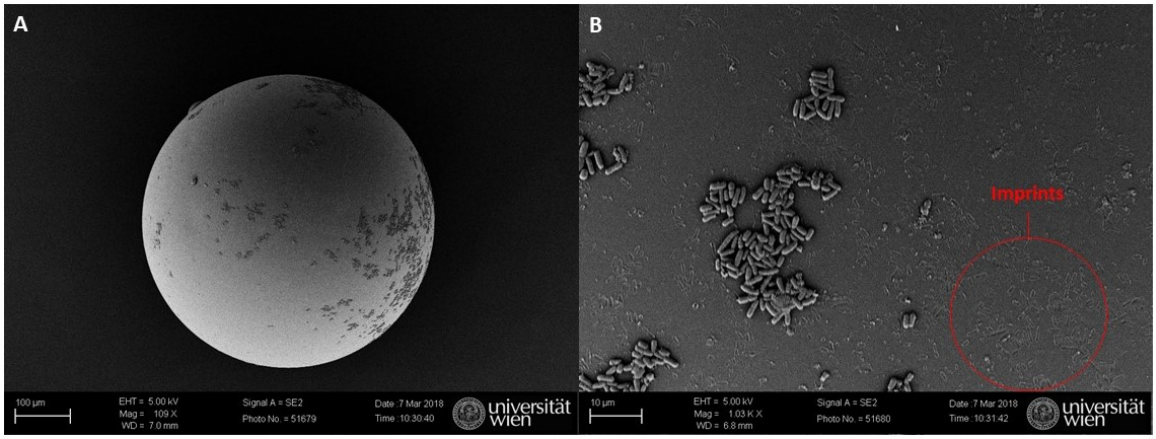

Figure 26: SEM image from a BIP-bead after the solvent extraction with 10% AcOH + 1% SDS, H_2O and methanol at 37°C: (A) image of the bead; (B) image of the bead surface (imprints are marked with red)

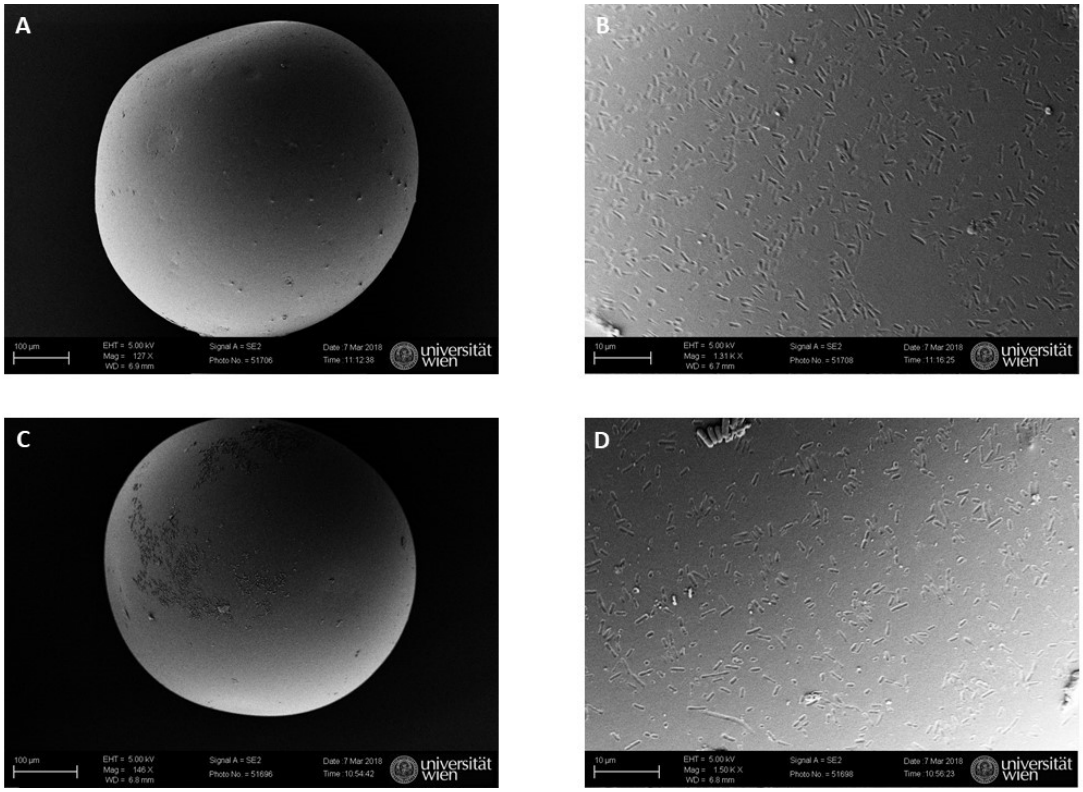

Figure 27: SEM images of BIP-beads after the solvent extraction with 10% AcOH + 1% SDS, H_2O and methanol at 0°C: (A) image of a BIP-bead where *E. coli* was completely removed ; (B) image of the beads surface where *E. coli* was completely removed; (C) image of a BIP-bead, were *E. coli* was partly removed; (D) image of the beads surface were *E. coli* was partly removed

The results of the solvent extraction experiments revealed that both approaches were feasible to remove *E. coli* almost completely from the surface of the BIP-beads. This indicates that applying shear forces over a longer extraction time drastically improves solvent extraction efficiency. Regarding the influence of temperature, it seems that the experiment performed at 0°C removed the bacteria more efficiently than the experiment carried out at 37°C.

All in all, BIP-beads washed by agitating for a distinct time in different extraction solvents provided a sufficient amount of cavities and left only few bacteria on the surface. This made them potentially useful materials for filtration and rebinding experiments with *E. coli*. However, the solvent extraction protocol could still be improved.

4.4.4. Increasing Extraction Time

In order to further improve extraction efficiency and to reduce the workload of the protocol, extraction time was drastically increased and the number of extraction steps was reduced. For this, only one extraction in 10% acetic acid + 1% SDS and methanol was carried out for 24 hours under agitation. The number of extraction steps in water remained the same as before (6 steps), but the extraction time was increased to 1 hour per step. The results of the BIP-bead examination with the SEM are illustrated in Figure 28.

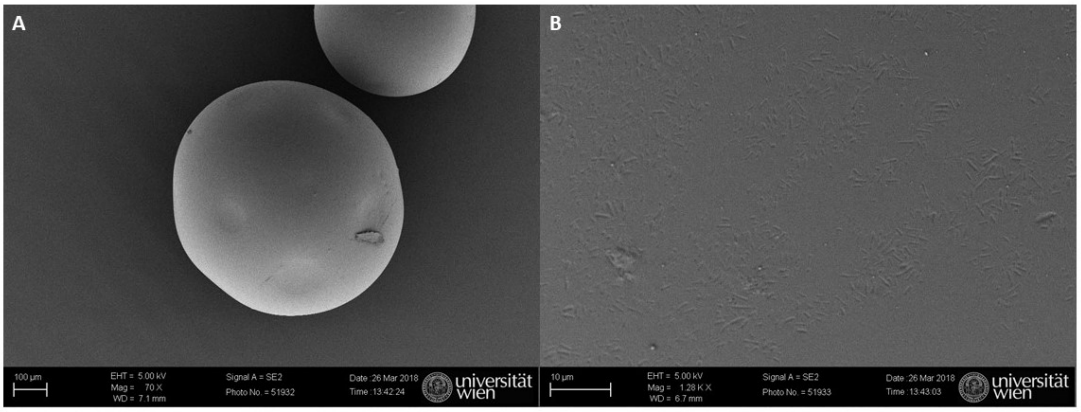

Figure 28: SEM Image of a BIP-bead after solvent extraction with increased extraction time (first step: 24h in 10% AcOH + 1% SDS; second step: 6x 1h in H_2O; third step: 24h in methanol): (A) image of the bead; (B) image of the beads surface

The results revealed that this long time solvent extraction approach is feasible to almost completely remove *E. coli* from the surface of the beads. Reducing the number of washing steps did not negatively influence the efficiency of the process, which indicates that time is more important than the number of extractions.

Investigation of the washing solutions under the light microscope revealed that most of the bacteria were extracted in 10% acetic acid + 1% SDS. This clearly demonstrated that this extraction step is the most efficient one in the protocol.

With this solvent extraction protocol, a method was developed to remove *E. coli* from the BIP-beads. The resulting materials are potentially useful for selective rebinding of bacteria to the

imprinted cavities on the surface. All further experiments were carried out with BIP-beads processed with this optimized washing protocol.

4.4.5. Influence of BIP-bead Shape on Extraction Efficiency

During the solvent extraction experiments it became apparent that the efficiency of bacteria removal does not only depend on the respective protocol, but also on bead shape. Some of the synthesized beads were not spherical. Their surface featured dents, which probably derived from Pickering emulsion polymerization. *E. coli* cells located inside these dents resisted removing by solvent extraction. An example for such a BIP-bead is shown in Figure 29.

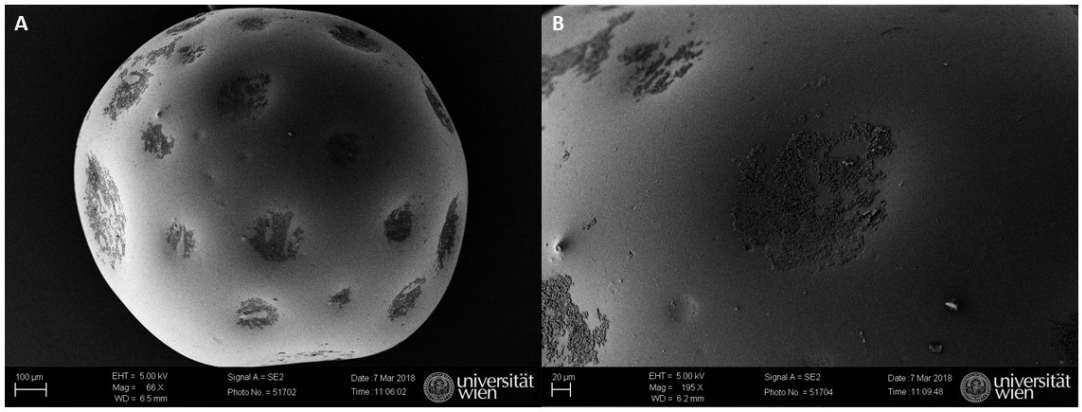

Figure 29: (A) SEM image of an extraction resistant BIP-bead; (B) SEM image of dents on the surface, occupied by *E. coli*

Interestingly, such abnormally shaped BIP-beads only appeared, if the diameter of the bead was ~ 800µm or higher. Therefore, it was possible to separate them from the smaller spherical beads by sieving. Hence, they did not distort the results of further experiments.

4.4.6. Solvent Extraction of BIP-beads synthesized in 0.1M PBS

As the entire solvent extraction optimization procedure was carried out with BIP-beads synthesized in water, the optimized protocol was also tested for the BIP-beads synthesized in 0.1M PBS. The results of the SEM investigations on these BIP-beads processed with the optimized solvent extraction protocol are illustrated in Figure 30.

Scanning electron microscopy revealed that indeed solvent extraction was also feasible to remove *E. coli* from the surface of 0.1M PBS polymerized BIP-beads, but there were far fewer imprints on their surfaces compared to those polymerized in water.

Generally speaking, imprints on BIP-beads were concentrated on distinct areas of the bead surface and hence did not entirely cover it. Additionally, such surfaces often revealed some deposited matter, probably arising from components of PBS.

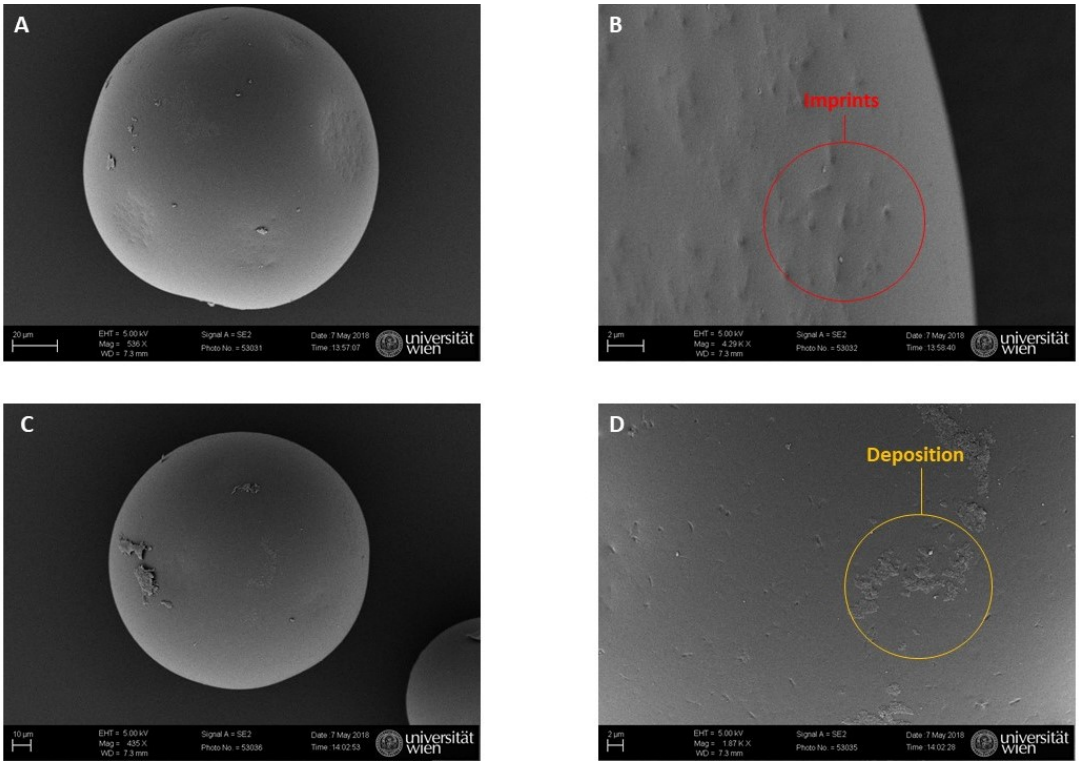

Figure 30: SEM images of BIP-beads polymerized in 0.1M PBS after solvent extraction: (A) BIP-bead with imprints concentrated on certain areas of the bead; (B) imprints on the BIP-bead (imprints are marked in red); (C) BIP-bead with depositions onto its surface; (D) depositions and imprints at the bead surface (depositions are marked in yellow)

4.4.7. Comparison of the two different BIP-bead types after solvent extraction

Both different types of BIP-beads (polymerized in water or 0.1M PBS) turned out potentially useful for rebinding and filtration of *E. coli*. However, their properties partly differ from one another. Therefore, they are more or less suitable for the following experiments. The SEM images of the two BIP-bead types in Figure 31 illustrate these differences:

It is clearly observable that BIP-beads polymerized in water feature a higher amount of imprints on their surfaces (Figure 31 B & D). This makes them more suitable to rebind *E. coli* into the cavities. As already mentioned before, bacteria preserved their size and shape during the Pickering emulsion polymerization in water (Figure 18 B). This was not the case for the

bacteria attached to BIP-beads polymerized in PBS (Figure 19 B). As the size of the cavities should fit to the bacteria to be attached, this favours the use of the BIP-beads polymerized in water. Therefore, they were the material of choice for the rebinding experiments.

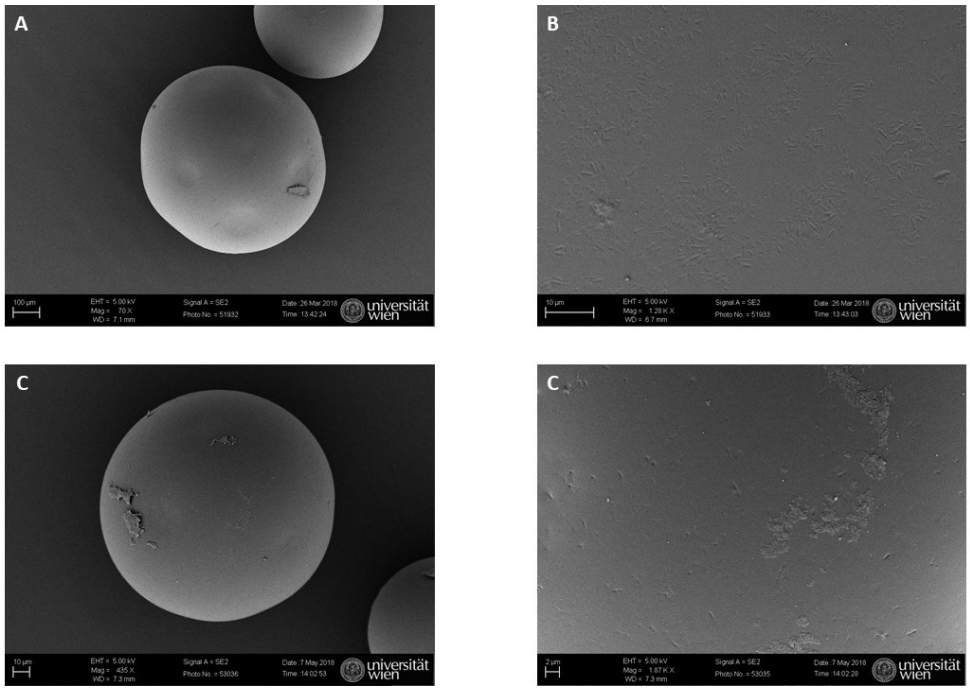

Figure 31: Comparison of the two different types of BIP-beads after solvent extraction: (A) BIP-bead polymerized in water; (B) imprints on the surface of beads polymerized in water; (C) BIP-beads polymerized in 0.1M PBS; (D) imprints on the surface of beads polymerized in 0.1M PBS

The main advantage of BIP-beads polymerized in PBS is their smaller size, which favours them to be used as column material for the filtration experiment. Even though they had fewer imprints onto their surface, a higher amount of beads could be used to pack the column. Smaller bead volume also results in a more compact column packing. Therefore, BIP-beads synthesized in PBS were the material of choice for filtration experiments.

4.5. *E. coli* Rebinding to the BIP-surface

4.5.1. Rebinding Experiments in 0.1M PBS

The ability of *E.coli* to rebind at the surface of BIP-beads after incubation in a bacteria suspension (3.2 x 10^8 CFU/mL; 0.1M PBS, pH=7.2) was examined under the SEM. The results are illustrated in Figure 32.

SEM revealed that the beads surface was loaded with *E. coli* and other deposed matter (Figure 32 B). Obviously, bacteria indeed rebind to the surface of the BIP-bead. The additional depositions probably derived from crystallized saline components of PBS.

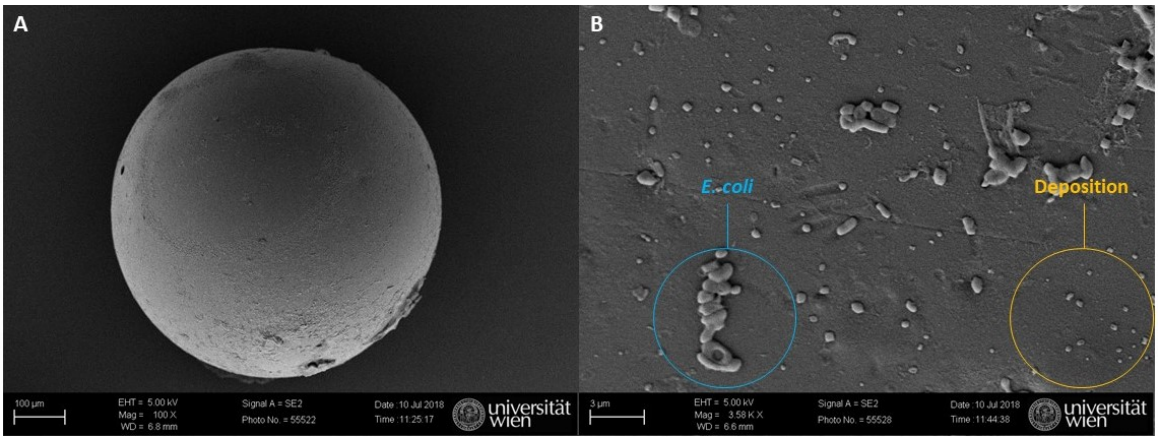

Figure 32: SEM image of a BIP-bead after incubation for 25h in an E. coli suspension (3.2 x 10^8 CFU/mL; 0.1M PBS, pH7.2): (A) image of the BIP-bead after incubation; (B) image of the bead surface after incubation (rebound *E. coli* are marked in blue; depositions are marked in yellow)

To determine whether bacteria are still bound to the BIP surface after washing with water, further SEM measurements were carried out on incubated beads after two washing steps with water. The results are illustrated in Figure 33.

They revealed that still a certain amount of *E. coli* was attached to the BIP-surface after washing. However, any deposited salt debris, disappeared after washing with water.

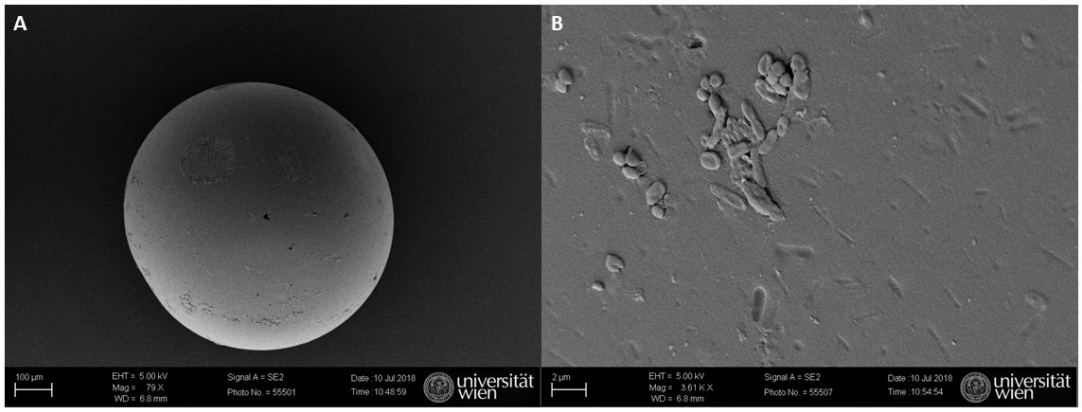

Figure 33: SEM image of a BIP-bead after incubation for 25h in an E. coli suspension (3.2 x 10^8 CFU/mL; 0.1M PBS, pH7.2); beads were washed with water after incubation: (A) image of the bead after incubation and washing; (B) image of the bead surface after incubation and washing

4.5.2. Rebinding Experiment in Water

The ability of *E.coli* to rebind at the surface of BIP-beads after incubation in a bacteria suspension (3.2 x 10^8 CFU/mL in water) was examined by SEM. The results are illustrated in Figure 34.

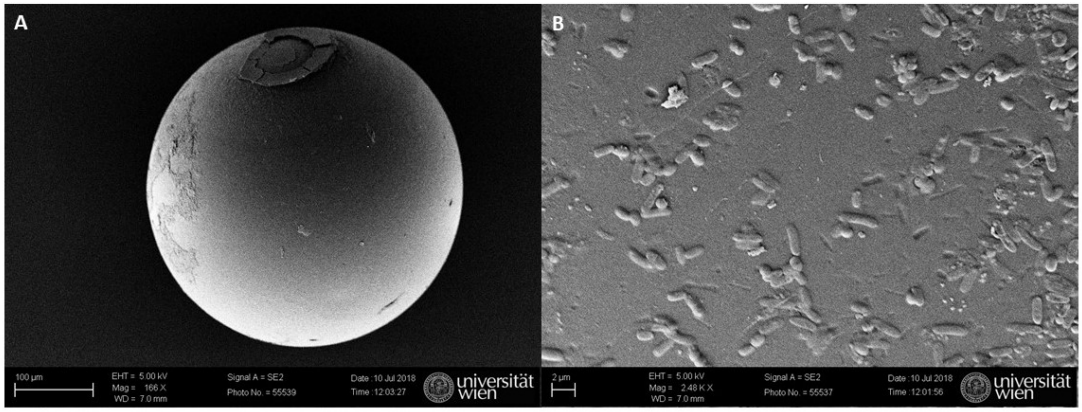

Figure 34: SEM image of a BIP-bead after incubation for 25h in an E. coli suspension (3.2 x 10^8 CFU/mL in water): (A) image of the bead after incubation; (B) image of the bead surface after incubation

It is obvious that bacteria bound to the BIP-surface during incubation. A further magnified SEM image revealed that *E. coli* cells are mainly located in the cavities resulting from imprinting (Figure 35).

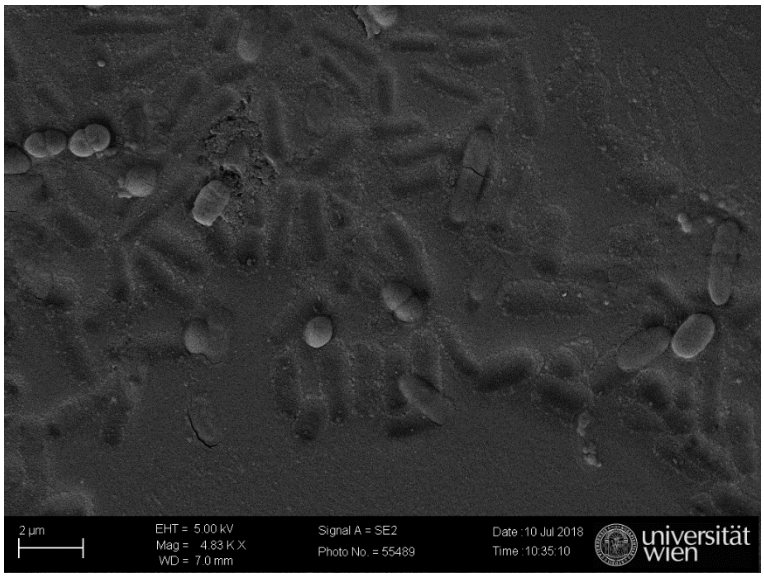

Figure 35: SEM image of *E. coli* located in the cavities of the BIP-beads; results were obtained from the rebinding experiment in an *E. coli* water suspension

The results of the rebinding experiments clearly demonstrated that the synthesized BIP-beads are potentially useful materials capable to bind *E. coli* onto their surface. For this, they are of interest for filtration or pre-concentration processes of this faecal indicator bacterium.

4.6. Filtration Experiments

Filtration experiments with bead-packed columns were coupled with a QCM sensor for *E. coli* to determine the filtration efficiency of both BIP and NIP beads.

4.6.1. Assessment of the Sensor Performance

First, the performance of the manufactured *E. coli*-sensitive QCM sensor was determined by calibration. For this, the sensor response was measured for a bacteria concentration range of 8 x 10^8 CFU/mL to 8 x 10^7 CFU/mL. During data processing, the entire data set was normalized around the first measured frequency of each electrode. The results are illustrated in Figure 36.

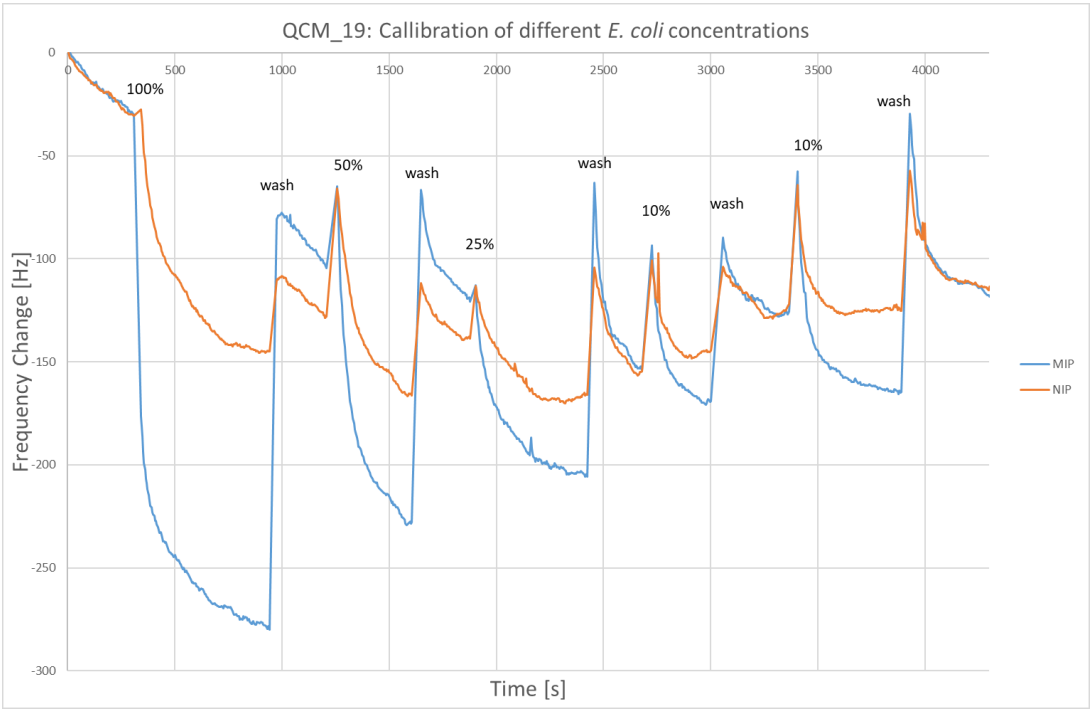

Figure 36: Calibration of *E. coli* concentration in the range of 8 x 10^8 CFU/mL to 8 x 10^7 CFU/mL; 100% corresponds to the bacteria concentration of 8 x 10^8 CFU/mL; the signals of the MIP-electrode (blue) and the NIP-electrode (orange) are illustrated in the diagram

This measurement revealed continuous drift independent from analyte concentration. However, MIP- and NIP- coated electrodes yielded significantly different frequency shifts. The difference depends on analyte concentration and was used for calibrating the *E. coli* sensor. The corresponding sensor signal can be seen in Figure 37.

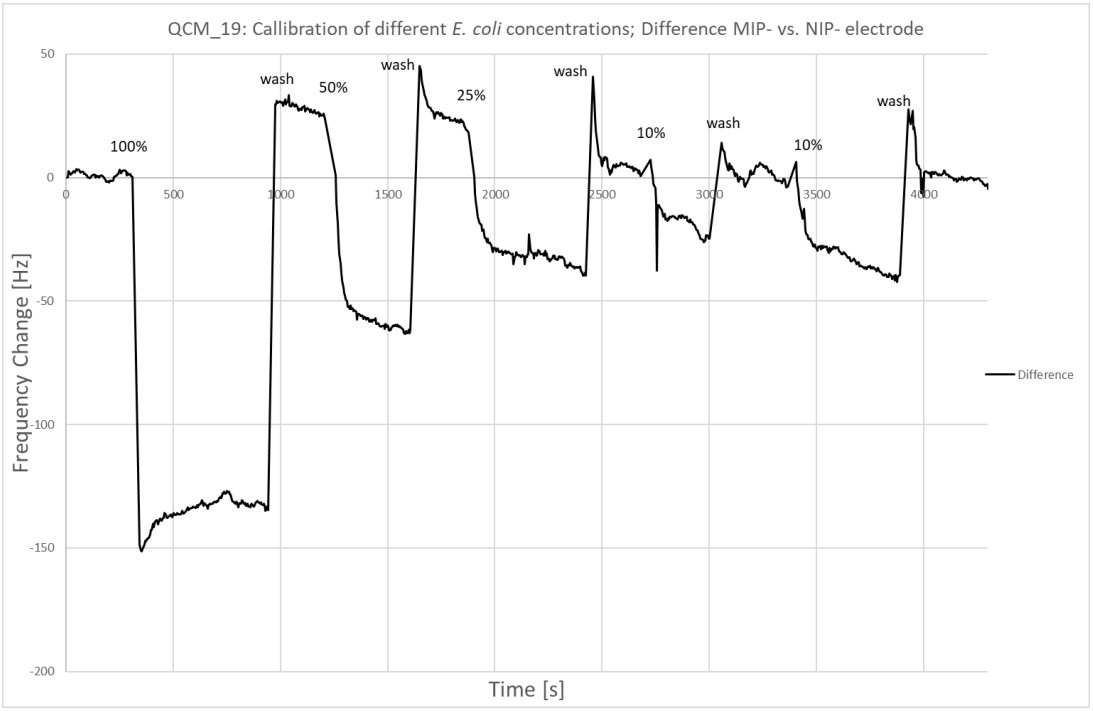

Figure 37: Calibration of *E. coli* concentration in the range of 8 x 10^8 CFU/mL to 8 x 10^7 CFU/mL; 100% corresponds to the bacteria concentration of 8 x 10^8 CFU/mL; the difference between the MIP- electrode and the NIP- electrode is illustrated in the diagram

To determine the signal caused by the respective *E. coli* suspension, the mean of the last 10 data points before injecting the sample was subtracted from the mean of the last 10 data points before the wash out. The results of this calibration are listed in Table 10 and Figure 38.

Table 10: Calibration of different *E. coli* concentrations with QCM_19; signal was determined via the difference of the MIP- to the NIP- electrode

c(*E. coli*) [10^8 CFU/mL]	8	4	2	0.8	0.8
Signal [-Hz]	135	88	59	28	38

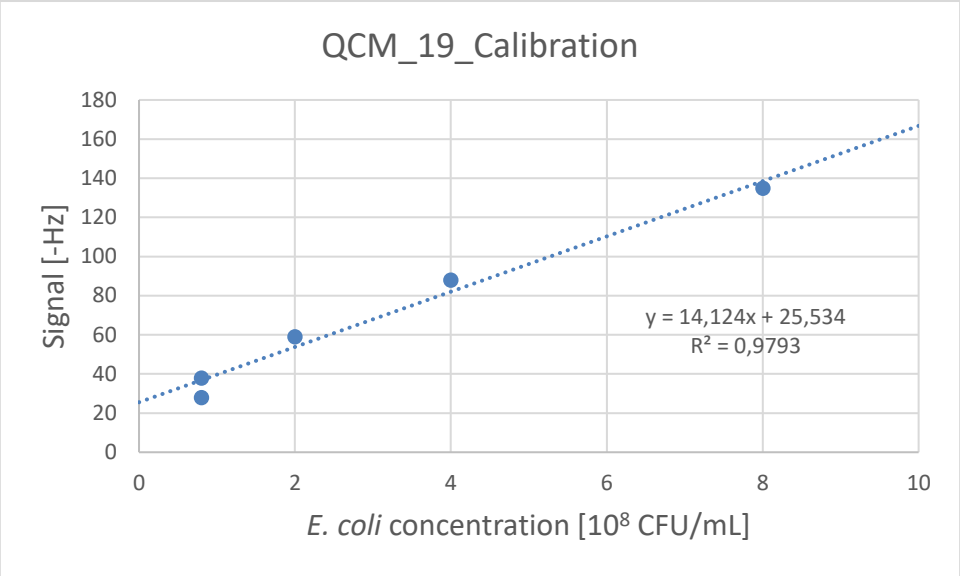

Figure 38: Calibration curve for different *E. coli* concentrations with QCM_19; signal was determined via the difference of the MIP- to the NIP- electrode

The results revealed that the manufactured QCM_19, was feasible to generate *E. coli* concentration dependent signals in the range between 8 x 10^8 CFU/mL to 8 x 10^7 CFU/mL. In this range, the sensor response featured approximately linear behaviour. Hence it was decided, to use QCM_19 for the determination of the extraction efficiency of the BIP-beads. The confidence level of 4.2Hz was determined as the three-fold noise of the first 50 data points.

4.6.2. Assessing the Filtration Efficiency of BIP

The examination of the filtration efficiency was performed with an *E. coli* solution of 2 x 10^8 CFU/mL. At the beginning, another calibration set of different bacteria concentration in the range between 2 x 10^8 CFU/mL to 8 x 10^7 CFU/mL was measured, right before the injection of the NIP- and BIP-bead filtrate. To overcome the analyte-independent frequency drift during the measurement, data were corrected with a linear following the equation bellow [56]:

$$f' = f - (a \cdot t)$$

With this, the original frequencies *f* were corrected by subtraction of a time dependent term, which consisted of a correction factor *a* multiplied with the time *t*. The obtained corrected frequencies *f'* had a lower analyte independent frequency drift as the original data. The

correction factor *a* was defined as the slope of the first 100 data points and was separately determined for both measuring electrodes. The entire data set was normalized around the first measured frequency of each electrode. The results of the filtration efficiency experiments, measured with the *E. coli* sensitive QCM_19, are illustrated in Figure 39.

The obtained frequency shifts for the measured filtrates were generally higher than the signals measured at the maximal *E. coli* concentration of 2 x 10^8 CFU/mL. Hence these first results were not useful to gain information about the filtration efficiency of the beads. Interestingly, the frequency shifts after extraction of the NIP-bead filtrate were higher as those of the BIP-bead filtrate.

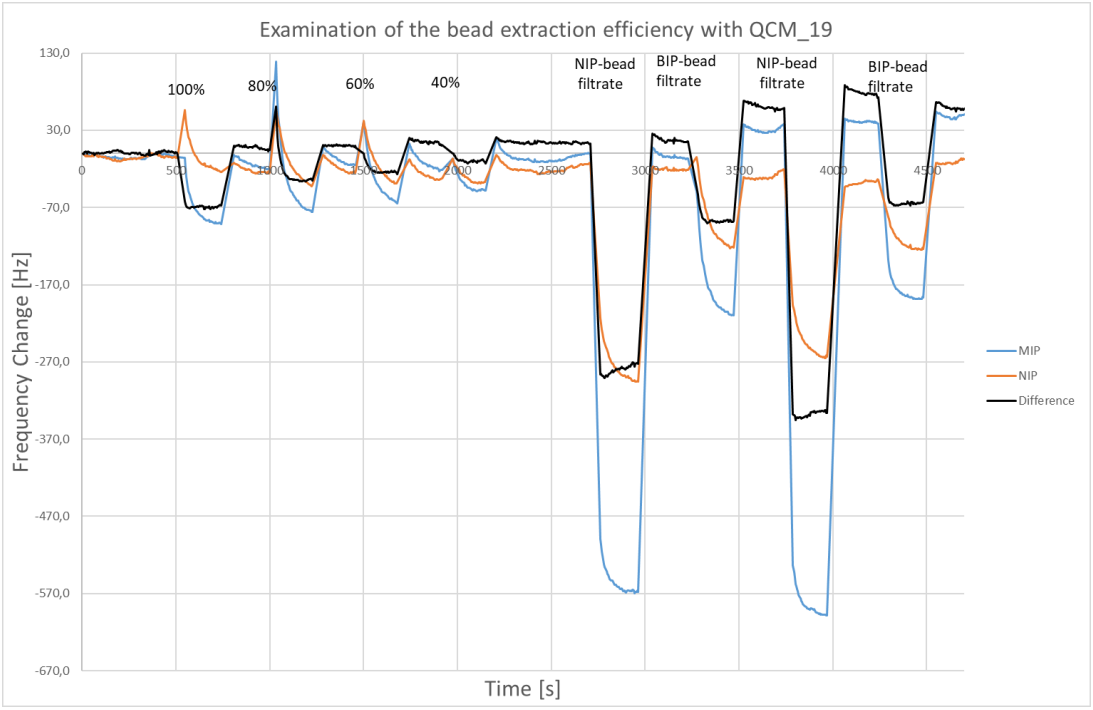

Figure 39: QCM_19 examination of the extraction efficiency of BIP-beads and NIP-beads; the measuring series consisted of a calibration set in the range between 2 x 10^8 CFU/mL to 8 x 10^7 CFU/mL followed by two injections of the BIP-bead filtrate and two injections of the NIP- bead filtrate; the processed signals of the MIP-electrode (blue), the NIP-electrode (orange) and the difference between the electrodes (black) are illustrated in the diagram

One possible explanation for the high signals obtained after bead filtration is that column material was flushed into the filtrate solution during the experiment. This assumption was confirmed by investigating the filtrate solution under the light microscope. An image of flushed column material is illustrated in Figure 40. As a QCM is a mass-sensitive measuring device, it is likely that column material (e.g. polystyrene bead shivers) induces frequency changes when deposited onto the electrodes. Such interferences made it impossible to examine filtration efficiency and therefore, this experiment setup was not feasible to determine the ability of the BIP-bead to filtrate *E. coli*. For this, it is appreciable to optimize

the experiment setup in further work, in order to examine the filtration efficiency of the BIP-beads.

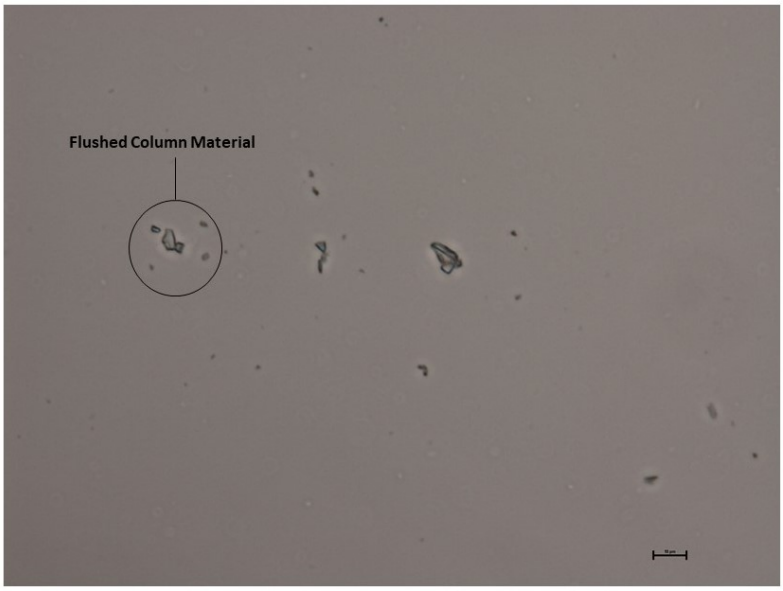

Figure 40: Light microscopy image of *E. coli* suspension filtrated through the BIP-column; flushed column material is marked with a black circle

4.7. *E. coli* Viability during the Pickering Emulsion Polymerization

To examine the ability of *E. coli* to stay viable during BIP-bead synthesis via a Pickering emulsion polymerization, different tests were carried out in varying aqueous phases. The viability of *E. coli* after polymerization was tested in the aqueous media, the washed BIP-beads and the dried BIP-beads. The results of the different approaches are listed in Table 11.

The results show that all viability tests were positive for Pickering emulsion polymerization in LB-medium as aqueous phase. The experiment was carried out four times, leading to the same results every time, which confirmed the repeatability of the experiment. All other approaches led only to negative outcome. Images of the positive viability tests on LB-Agar plates are illustrated in Figure 41.

Table 11: Results of the viability tests on LB-Agar plates for the different Pickering emulsion polymerization approaches

Approach	Viability Test (Aqueous Phase)	Viability Test (Washed Beads)	Viability Test (Dried Beads)
0.5mL Styrene 0.5mL DVB 18mg AIBN 1.2mL *E. coli* suspension in **water**	negative	negative	negative
0.5mL Styrene 0.5mL DVB 18mg AIBN 1.2mL *E. coli* suspension in **glucose solution (1g/L)**	negative	negative	negative
0.5mL Styrene 0.5mL DVB 18mg AIBN 1.2mL *E. coli* suspension in **LB-medium**	positive	positive	positive

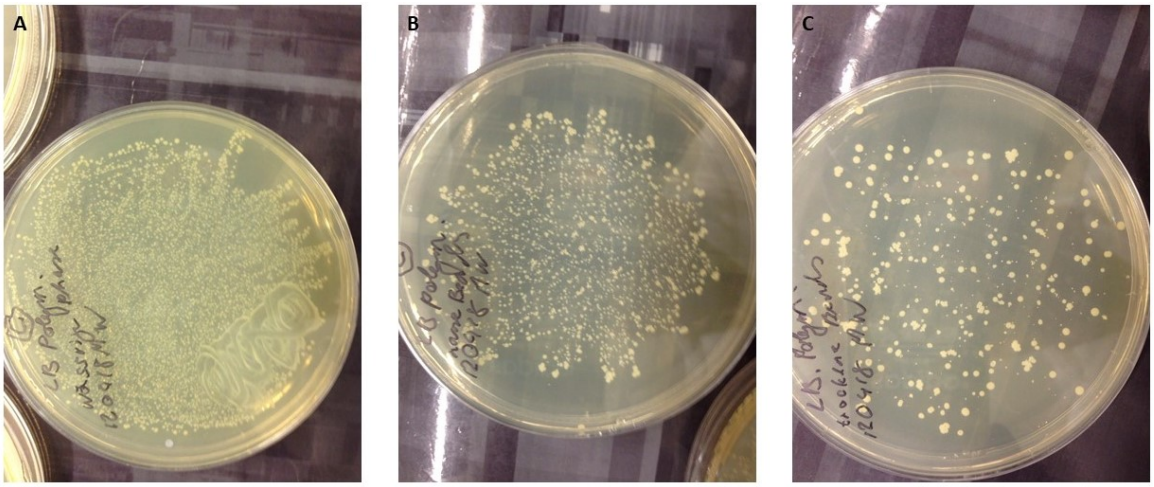

Figure 41: Images of positive viability tests for the Pickering emulsion polymerization in LB-medium: (A) picture of the positive test for the aqueous phase; (B) picture of the positive test for the washed beads; (C) picture of the positive test for the dried beads

The positive viability test for the aqueous phase and the washed beads revealed growing *E. coli* colonies all over the test plate after 24h incubation at 37°C. For the viability test with the washed beads, not only CFUs around the beads were observable. Therefore, it is likely that viable *E. coli* were also present in the remaining water of the washing solution.

The positive viability test for the dried beads revealed growing *E. coli* colonies around the beads spread onto the agar plates after 48h incubation at 37°C. As colonies were only formed

around the beads during this experiments, viability tests demonstrate that indeed the bacteria bound to the beads stayed viable.

To confirm that the CFUs derived from *E. coli*, Gram staining was performed. A light microscopy image of the stained bacteria, taken from a positive viability test, is illustrated in Figure 42.

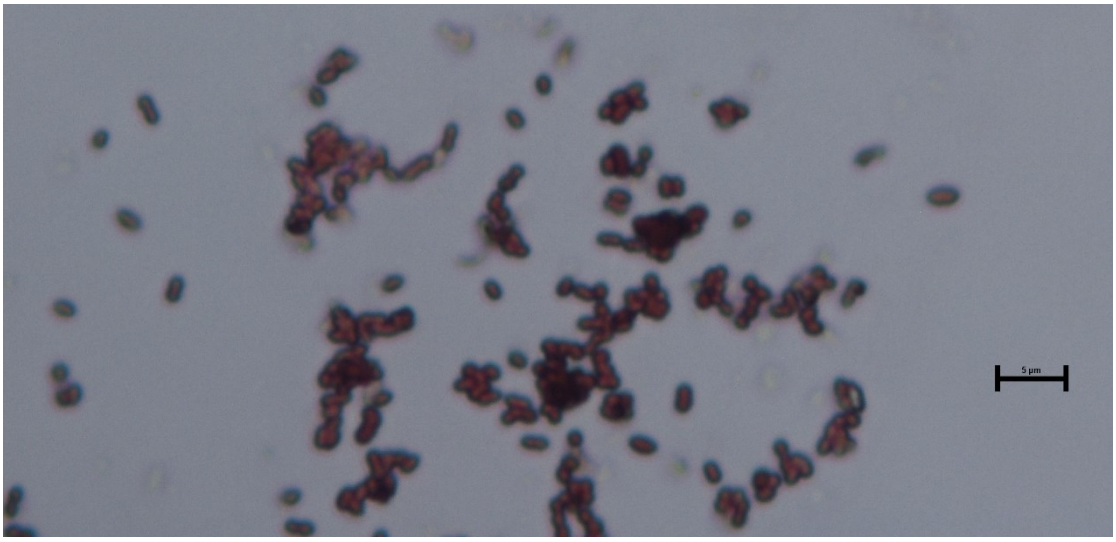

Figure 42: Light microscopy image of Gram stained bacteria, taken from a positive viability test of washed beads polymerized in LB medium as aqueous phase

Gram staining revealed that the bacteria grown on the agar plates of the positive viability tests, were rod shaped, Gram negative bacteria. No contaminations were observed. For this, the results confirmed that the grown bacteria were indeed *E. coli*. The fact that their size is smaller than normal indicated that the rather harsh conditions during Pickering emulsion polymerization had an impact on the shape of the bacteria. Nevertheless, they preserved their ability to proliferate, when they were exposed to the optimal growth conditions of the viability test. A change in cell size of *E. coli* as a response to unfavourable environmental conditions was already reported [60], which supports the assumption that the abnormal size was a result of the Pickering emulsion polymerization.

The ability of viable bacteria on the dried Beads to proliferate in LB- liquid medium was also examined. After 48 hours of incubation at 37°C, increased turbidity of the liquid culture was observable. Centrifugation of the liquid culture resulted in a bacteria pellet. Gram staining and investigation under the microscope revealed that the grown bacteria were *E. coli*. The results were comparable to the gram staining of the bacteria cultures on the positive LB- agar plates.

The results of the viability tests for the beads polymerized in LB-medium via Pickering emulsion polymerization thus revealed that *E. coli* was able to preserve a viable state during the synthesis of BIP-beads. With this, it was possible to produce beads with attached bacteria,

able to proliferate in beneficial environment. These materials could be used as transport devices for probiotics, which might be of interest for medical applications.

4.8. Investigation of the BIP-Bead Surface Polymerized in LB-Medium

The BIP-beads, which resulted in positive viability tests, were examined under the SEM. It was investigated, if the composition of the LB-medium and the fact that bacteria stayed viable during the polymerization, had an influence on the morphology of the bead surface. The results are illustrated in Figure 43.

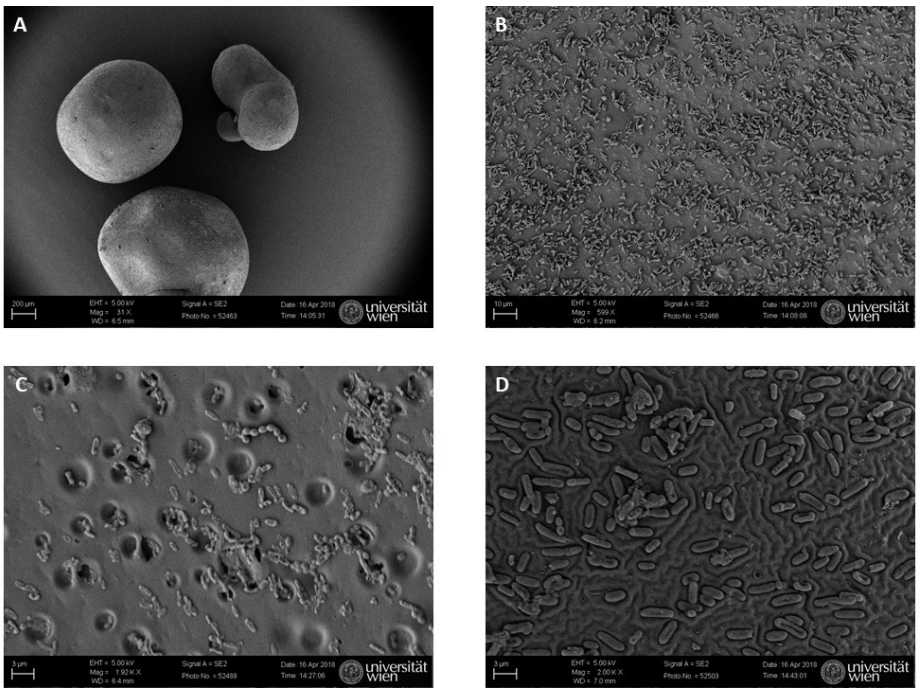

Figure 43: SEM images of BIP-beads polymerized in LB- liquid medium: (A) image illustrates the bead shape; (B-D) images illustrate different surface morphologies of the beads

Scanning electron microscopy shows that the shape of these BIP-beads was not utterly spherical. *E. coli* was located all over the surface of the beads. Closer investigation of the surface morphology revealed alterations compared to the previous investigated BIP-beads polymerized in water or PBS. Circular holes, inhabited by bacteria, were observable at certain parts of the bead surface (Figure 43 C). On other areas, groves determined the morphology of the beads (Figure 43 D). *E. coli* bacteria were embedded in those groves, which gives raise to the assumption that this special morphology might occur due to bacteria movement during the formation of the BIP-bead. However, it could not be clarified whether the viability of the

bacteria or possible surface-active compounds in the LB-medium were responsible for the alteration of the bead shape and morphology.

5. Conclusion

To sum up, BIP-bead synthesis at 37°C via a Pickering emulsion polymerization was successful when using 2wt% AIBN as initiator of the free radical polymerization of styrene and DVB. *E. coli* bound to the surface of the generated material could be effectively removed by an optimized solvent extraction protocol. It was possible to identify the temperature, the extraction time and the applying of shear forces as influence factors for a successful solvent extraction. The best results were obtained with 24 hours solvent extraction in 10% acetic acid + 1% SDS, followed by six solvent extractions in water (each of them one hour) and 24 hours solvent extraction in methanol. Shear forces were applied by agitation of the beads in the extraction solvent. With this, polystyrene beads featuring cavities in the shape and size of *E. coli* were manufactured. Their inherent ability to rebind *E. coli* into the imprints was demonstrated in several experiments, based on bead incubation in *E. coli* suspensions and subsequent surface investigations with the SEM. It also became clear that the bead size could be reduced by increasing the ionic strength of the aqueous phase during the Pickering emulsion polymerization. BIP-beads synthesized in 0.1M PBS instead of water featured an overall smaller size than those polymerized in water. This was crucial for their usability as column material in the filtration experiments.

The manufacturing of an *E. coli* sensitive QCM-MIP-sensor, which was based on a previously optimized protocol [56], could be reproduced. Sensitivity was generated via stamp imprinting of a Poly(2-(hydroxyethyl)methacrylate-co-N,N'-ethylenebisacrylamide) layer on the quartz electrode. However, the coupling of the sensor with a BIP-bead column was not able to determine the filtration efficiency of the beads, due to complications derived from the flushing of column material onto the QCM-sensor. For this, further work, focusing on the optimization of the experiment setup, is needed. In future work, it would be appreciable to establish a setup, which combines a pre-concentration column, consisting of the BIP-beads, with an *E. coli* sensor. Such a measuring device would be inherently promising to feature a high sensitivity, due to the pre-concentration step and a high selectivity generated via two different MIP materials.

Apart from the examined applications of BIP-bead for the detection of *E. coli*, it was possible to demonstrate that the beads might also be useful as microorganism transport devices, as the synthesis of BIP-beads with *E. coli* that preserved its viability, was successful. The crucial factor that ensured the survival of the bacteria during the harsh conditions of the Pickering emulsion polymerization was the use of LB-liquid medium as aqueous phase. Beads with viable bacteria bound onto their surface open up new possibilities for the administration of probiotics, which could be of interest for medical applications. However, further experiments are needed to examine possible risks and benefits of BIP-beads as microorganism transport devices.

6. References

[1] C. Gradmann, “Robert Koch and the white death: From tuberculosis to tuberculin,” *Microbes Infect.*, vol. 8, no. 1, pp. 294–301, 2006.

[2] A. De Brauwere, N. K. Ouattara, and P. Servais, “Modeling fecal indicator bacteria concentrations in natural surface waters: A review,” *Crit. Rev. Environ. Sci. Technol.*, vol. 44, no. 21, pp. 2380–2453, 2014.

[3] WHO (World Health Organization), “Waterborne disease related to unsafe water and sanitation,” 2018. [Online]. Available: http://www.who.int/sustainable-development/housing/health-risks/waterborne-disease/en/. [Accessed: 31-Jul-2018].

[4] V. Dixit, J. C. Tewari, and B. S. Sharma, “Detection of E. coli in water using semi-conducting polymeric thin film sensor,” *Sensors Actuators, B*, vol. 120, no. 1, pp. 96–103, 2006.

[5] WHO (World Health Organization), “A global overview of national regulations and standards for drinking-water quality,” Geneva, 2018.

[6] A. Beltran, F. Borrull, R. M. Marcé, and P. A. G. Cormack, “Molecularly-imprinted polymers: Useful sorbents for selective extractions,” *TrAC - Trends Anal. Chem.*, vol. 29, no. 11, pp. 1363–1375, 2010.

[7] X. Shen *et al.*, “Bacterial imprinting at pickering emulsion interfaces,” *Angew. Chemie - Int. Ed.*, vol. 53, no. 40, pp. 10687–10690, 2014.

[8] F. G. Tamayo, E. Turiel, and A. Martín-Esteban, “Molecularly imprinted polymers for solid-phase extraction and solid-phase microextraction: Recent developments and future trends,” *J. Chromatogr. A*, vol. 1152, no. 1–2, pp. 32–40, 2007.

[9] C. S. Chern, “Emulsion polymerization mechanisms and kinetics,” *Prog. Polym. Sci.*, vol. 31, no. 5, pp. 443–486, 2006.

[10] F. L. Dickert, O. Hayden, and K. P. Halikias, “Synthetic receptors as sensor coatings for molecules and living cells,” *Analyst*, vol. 126, no. 6, pp. 766–771, 2001.

[11] M. Werner, J. Perko, V. Prinz, A. Bismarck, and P. A. Lieberzeit, “Pickering Emulsion Polymerization of Polystyrene to Synthesize Bacteria Imprinted Polymer Beads for Pre-Concentration,” in *17th International Meeting on Chemical Sensors - IMCS 2018*, 2018, pp. 699–700.

[12] S. Fijan, “Microorganisms with claimed probiotic properties: An overview of recent literature,” *Int. J. Environ. Res. Public Health*, vol. 11, no. 5, pp. 4745–4767, 2014.

[13] P. J. Dowding and B. Vincent, “Suspension polymerisation to form polymer beads,” *Colloids Surfaces A Physicochem. Eng. Asp.*, vol. 161, no. 2, pp. 259–269, 2000.

[14] E. Piskin, A. Tuncel, A. Denizli, and H. Ayhan, “Monosize microbeads based on polystyrene and their modified forms for some selected medical and biological applications,” *J. Biomater. Sci. Polym. Ed.*, vol. 5, no. 5, pp. 451–471, 1994.

[15] Y. Chevalier and M. A. Bolzinger, “Emulsions stabilized with solid nanoparticles: Pickering emulsions,” *Colloids Surfaces A Physicochem. Eng. Asp.*, vol. 439, pp. 23–34, 2013.

[16] K. Roger, U. Olsson, R. Schweins, and B. Cabane, “Emulsion ripening through molecular exchange at droplet contacts,” *Angew. Chemie - Int. Ed.*, vol. 54, no. 5, pp. 1452–1455, 2015.

[17] Y. Meliana, L. Suprianti, Y. C. Huang, C. T. Lin, and C. S. Chern, “Effect of mixed costabilizers on Ostwald ripening of monomer miniemulsions,” *Colloids Surfaces A Physicochem. Eng. Asp.*, vol. 389, no. 1–3, pp. 76–81, 2011.

[18] X. Shen and L. Ye, “Interfacial molecular imprinting in nanoparticle-stabilized emulsions,” *Macromolecules*, vol. 44, no. 14, pp. 5631–5637, 2011.

[19] J. van Wijk, T. Heunis, E. Harmzen, L. M. T. Dicks, J. Meuldijk, and B. Klumperman, “Compartmentalization of bacteria in microcapsules,” *Chem. Commun.*, vol. 50, no. 97, pp. 15427–15430, 2014.

[20] S. R. Sandler, *Polymer Synthesis and Characterization : A Laboratory Manual*. San Diego: Academic Press, 1998.

[21] M. Buback, B. Huckestein, F. -D Kuchta, G. T. Russell, and E. Schmid, “Initiator efficiencies in 2,2’-azoisobutyronitrile-initiated free-radical polymerizations of styrene,” *Macromol. Chem. Phys.*, vol. 195, no. 6, pp. 2117–2140, 1994.

[22] W. Kangwansupamonkon, S. Damronglerd, and S. Kiatkamjornwong, “Effects of the crosslinking agent and diluents on bead properties of styrene-divinylbenzene copolymers,” *J. Appl. Polym. Sci.*, vol. 85, no. 3, pp. 654–669, 2002.

[23] M. Hussain, J. Wackerlig, and P. A. Lieberzeit, “Biomimetic strategies for sensing biological species,” *Biosensors*, vol. 3, no. 1, pp. 89–107, 2013.

[24] I. A. Nicholls and J. P. Rosengren, “Molecular imprinting of surfaces,” *Bioseparation*, vol. 10, no. 6, pp. 301–305, 2002.

[25] E. Turiel and A. Martín-Esteban, “Molecularly imprinted polymers for sample preparation: A review,” *Anal. Chim. Acta*, vol. 668, no. 2, pp. 87–99, 2010.

[26] C. J. Tan and Y. W. Tong, “Molecularly imprinted beads by surface imprinting,” *Anal. Bioanal. Chem.*, vol. 389, no. 2, pp. 369–376, 2007.

[27] E. Spieker and P. A. Lieberzeit, “Molecular Imprinting Studies for Developing QCM-sensors for Bacillus Cereus,” *Procedia Eng.*, vol. 168, pp. 561–564, 2016.

[28] T. Cohen, J. Starosvetsky, U. Cheruti, and R. Armon, “Whole cell imprinting in sol-gel thin films for bacterial recognition in liquids: Macromolecular fingerprinting,” *Int. J. Mol. Sci.*, vol. 11, no. 4, pp. 1236–1252, 2010.

[29] T. Zhou, K. Zhang, T. Kamra, L. Bülow, and L. Ye, “Preparation of protein imprinted polymer beads by Pickering emulsion polymerization,” *J. Mater. Chem. B*, vol. 3, no. 7, pp. 1254–1260, 2015.

[30] X. Shen and L. Ye, “Molecular imprinting in Pickering emulsions: a new insight into molecular recognition in water,” *Chem. Commun.*, vol. 47, no. 37, pp. 10359–10361, 2011.

[31] T. Zhou, T. Kamra, and L. Ye, “Preparation of diclofenac-imprinted polymer beads for selective molecular separation in water,” *J. Mol. Recognit.*, vol. 31, no. 3, pp. 1–7, 2018.

[32] G. Ertürk and B. Mattiasson, “Molecular imprinting techniques used for the preparation of biosensors,” *Sensors*, vol. 17, no. 2, pp. 1–17, 2017.

[33] S. Li, S. Cao, M. J. Whitcombe, and S. A. Piletsky, “Size matters: Challenges in imprinting macromolecules,” *Prog. Polym. Sci.*, vol. 39, no. 1, pp. 145–163, 2014.

[34] F.-G. Banica, *Chemical Sensors and Biosensors: Fundamentals and Applications*, 1st ed. Chichester: John Wiley & Sons, Ltd., 2012.

[35] J. Tamayo, P. M. Kosaka, J. J. Ruz, Á. San Paulo, and M. Calleja, “Biosensors based on nanomechanical systems,” *Chem. Soc. Rev.*, vol. 42, no. 3, pp. 1287–1311, 2013.

[36] K. Haupt and K. Mosbach, “Molecularly imprinted polymers and their use in biomimetic sensors,” *Chem. Rev.*, vol. 100, no. 7, pp. 2495–2504, 2000.

[37] C. K. O’Sullivan and G. G. Guilbault, “Commercial quartz crystal microbalances - Theory and applications,” *Biosens. Bioelectron.*, vol. 14, no. 8–9, pp. 663–670, 1999.

[38] G. Sauerbrey, “Verwendung von Schwingquarzen zur Wägung dünner Schichten und zur Mikrowägung,” *Zeitschrift für Phys.*, vol. 155, no. 2, pp. 206–222, 1959.

[39] J. A. Botha *et al.*, “Quartz crystal microbalance as a device to measure the yield stress of colloidal suspensions,” *Colloids Surfaces A Physicochem. Eng. Asp.*, vol. 546, pp. 179–185, 2018.

[40] W. Tao, P. Lin, Y. Ai, H. Wang, S. Ke, and X. Zeng, “Multichannel quartz crystal microbalance array: Fabrication, evaluation, application in biomarker detection,” *Anal. Biochem.*, vol. 494, pp. 85–92, 2016.

[41] Z. Iskierko, P. S. Sharma, K. Bartold, A. Pietrzyk-Le, K. Noworyta, and W. Kutner, “Molecularly imprinted polymers for separating and sensing of macromolecular compounds and microorganisms,” *Biotechnol. Adv.*, vol. 34, no. 1, pp. 30–46, 2016.

[42] M. Cieplak and W. Kutner, “Artificial Biosensors: How Can Molecular Imprinting Mimic Biorecognition?,” *Trends Biotechnol.*, vol. 34, no. 11, pp. 922–941, 2016.

[43] M. Panagiotopoulou, S. Beyazit, S. Nestora, K. Haupt, and B. Tse Sum Bui, “Initiator-free synthesis of molecularly imprinted polymers by polymerization of self-initiated monomers,” *Polym. (United Kingdom)*, vol. 66, pp. 43–51, 2015.

[44] T. A. T. Gomes *et al.*, “Diarrheagenic Escherichia coli,” *Brazilian J. Microbiol.*, vol. 47, pp. 3–30, 2016.

[45] G. Reshes, S. Vanounou, I. Fishov, and M. Feingold, “Cell shape dynamics in

Escherichia coli," *Biophys. J.*, vol. 94, no. 1, pp. 251–264, 2008.

[46] C. T. Archer *et al.*, "The genome sequence of E. coli W (ATCC 9637): Comparative genome analysis and an improved genome-scale reconstruction of E. coli," *BMC Genomics*, vol. 12, no. 1, p. 9, 2011.

[47] O. Rotariu *et al.*, "Combining risk assessment and epidemiological risk factors to elucidate the sources of human E. coli O157 infection," *Epidemiol. Infect.*, vol. 140, no. 8, pp. 1414–1429, 2012.

[48] T. M. Wassenaar, "Insights from 100 years of research with probiotic *E. coli*," *Eur. J. Microbiol. Immunol.*, vol. 6, no. 3, pp. 147–161, 2016.

[49] K. D. Vernon-Parry, "Scanning electron microscopy: an introduction," *III-Vs Rev.*, vol. 13, no. 4, pp. 40–44, 2000.

[50] C. Ngô and M. H. Van de Voorde, *Nanotechnology in a Nutshell: From Simple to Complex Systems*. Paris: Atlantis Press, 2014.

[51] S. Amelinckx, D. Van Dyck, J. Van Landuyt, and G. Van Tendeloo, *Electron Microscopy: Principles and Fundamentals*. Weinheim: VCH Verlagsgesellschaft mbH, 1997.

[52] R. B. Bolon, "Inexpensive dc sputtering system for scanning electron microscopy," *Rev. Sci. Instrum.*, vol. 46, no. 10, pp. 1421–1422, 1975.

[53] M. Otto, *Analytische Chemie*, 4th ed. Weinheim: WILEY-VCH GmbH & Co. KGaA, 2011.

[54] G. Schwedt, *Analytische Chemie Grundlagen, Methoden und Praxis*, 2nd ed. Weinheim: WILEY-VCH GmbH & Co. KGaA, 2008.

[55] A. J. Pasquale and T. E. Long, "Real-Time Monitoring of the Stable Free Radical Polymerization of Styrene via in-Situ Mid-Infrared Spectroscopy," *Macromolecules*, vol. 32, no. 23, pp. 7954–7957, 1999.

[56] J. M. Westermayr, "Modern UV-induced polymerization approaches for synthesizing Escherichia coli molecularly imprinted polymers," University of Vienna, 2017.

[57] H. Yu, Y. Fang, L. Chen, and S. Chen, "Investigation of redox initiators for free radical frontal polymerization," *Polym. Int.*, vol. 58, no. 8, pp. 851–857, 2009.

[58] M. Antonietti and K. Landfester, "Polyreactions in miniemulsions," *Prog. Polym. Sci.*, vol. 27, no. 4, pp. 689–757, 2002.

[59] N. Girard, T. F. Tadros, and A. I. Bailey, "Polymerization of oil (styrene and methylmethacrylate) in water microemulsions," *Colloid Polym. Sci.*, vol. 276, no. 11, pp. 999–1009, 1998.

[60] T. Pilizota and J. W. Shaevitz, "Plasmolysis and cell shape depend on solute outer-membrane permeability during hyperosmotic shock in E. coli," *Biophys. J.*, vol. 104, no. 12, pp. 2733–2742, 2013.

7. Appendix

7.1. Abstract

Enumerating *E. coli* is used to predict the sanitary risk in water: This bacterium is an indicator for fecal contaminations. However, established analysis methods are usually time-consuming and expensive. Therefore, the development of chemical sensors for detecting *E. coli* is of interest. Such measuring devices require high sensitivity to determine fecal contaminations in real water samples. Materials capable for selectively binding *E. coli* could help to improve sensitivity of the sensor, as they can be exploited for filtration and pre-concentration previously to sensing of the bacterium. In this work, BIP-beads were synthesized via a Pickering emulsion polymerization of styrene and DVB. In this process, *E. coli* functioned as a stabilizer of the emulsion and as the template for molecular imprinting. With AIBN as initiator, poly(styrene-co-divinylbenzene)-beads could be synthesized at 37°C. The obtained BIP-beads were processed with solvent extractions based on acetic acid, SDS, water and methanol, which removed the bacteria effectively from the surface leaving imprints in the shape and size of *E. coli* behind. The optimized solvent extraction protocol consisted of 24 hours washing in 10% acetic acid + 1% SDS, followed by six extraction steps in water (each 1 hour) and 24 hours washing in methanol. BIP-beads were agitated in the respective solutions during the whole process. The developed material featured the ability to rebind *E. coli* onto its surface. For this, the use of BIP-beads for filtration and pre-concentration is promising to support the monitoring of *E. coli* in water. Further, it was demonstrated that a Pickering emulsion polymerization with LB-medium as aqueous phase, assured the viability of the bacteria during the polymerization.

7.2. Zusammenfassung

Die Bestimmung der *E. coli* Konzentration wird verwendet um das Gesundheitsrisiko von Wasser vorherzusagen, da dieses Bakterium auf Kontaminationen durch Fäkalien hinweist. Die etablierten Analysemethoden sind in der Regel zeitintensiv und teuer, weshalb die Entwicklung von chemischen Sensoren, welche für die Detektion von *E. coli* geeignet sind, von großem Interesse ist. Um Fäkalkontaminationen in realen Wasserproben zu detektieren muss das Messgeräte jedoch eine hohe Sensitivität aufweisen. Materialien, welche die Fähigkeit besitzen *E. coli* selektiv zu binden, könnten die Sensitivität eines Sensors verbessern, da sie zur Filtration und Vorkonzentration verwendet werden könnten. Im Zuge dieser Arbeit wurden BIP-Beads durch die Pickering Emulsionspolymerisation von Styren und DVB synthetisiert. Dabei diente *E. coli* sowohl als Stabilisator der Emulsion als auch als Templat für das molekulare Prägen. Die Synthese von Poly(Styren-co-Divynilybenzen)-Beads konnte durch die Verwendung des Initiators AIBN bei 37°C realisiert werden. Die Bakterien auf der Oberfläche der BIP-Beads konnten durch Lösungsmittel Extraktionen, basierend auf Essigsäure, SDS, Wasser und Methanol, effizient entfernt werden, wodurch Kavitäten in der Größe und Form von *E. coli* sichtbar wurden. Das optimierte Extraktionsprotokoll bestand aus einem 24 stündigem Waschschritt in 10% Essigsäure + 1% SDS, gefolgt von sechs Extraktionen in Wasser (je 1 Stunde) und einem 24 stündigem Waschschritt in Methanol. Die BIP-Beads wurden während des ganze Extraktionsvorgangs in der jeweiligen Waschlösung aufgewirbelt. Das entwickelte Material erwies sich als fähig, *E. coli* erneut auf seiner Oberfläche zu binden. Daher sind BIP-Beads vielversprechende Sorbenzien für Filtrationen und Vorkonzentrierung, wodurch die Überwachung der *E. coli* Konzentration in Wasser verbessert werden könnte. Des Weiteren wurde gezeigt, dass es möglich ist, *E. coli* während der Pickering Emulsionspolymerisation in einem lebensfähigen Zustand zu halten. Dabei wurden die BIP-Beads in einer Suspension aus Bakterien in LB Nährmedium synthetisiert.